Performance Analysis and Mitigation Techniques for I/Q-Corrupted OFDM Systems

Udesh Oruthota

Aalto University

DOCTORAL DISSERTATIONS

Aalto University publication series
DOCTORAL DISSERTATIONS 219/2015

Performance Analysis and Mitigation Techniques for I/Q-Corrupted OFDM Systems

Udesh Oruthota

A doctoral dissertation completed for the degree of Doctor of Science (Technology) to be defended, with the permission of the Aalto University School of Electrical Engineering, at a public examination held at the lecture hall S1 of the school on 15 January 2016 at 12 noon.

Aalto University
School of Electrical Engineering
Department of Communications and Networking

Supervising professor
Prof. Olav Tirkkonen, Aalto University, Finland

Preliminary examiners
Prof. Mats Bengtsson, KTH Royal Institute of Technology, Sweden
Dr. Michail Matthaiou, Queen's University, United Kingdom

Opponent
Prof. Tommy Svensson, Chalmers University, Sweden

Aalto University publication series
DOCTORAL DISSERTATIONS 219/2015

ISBN 978-952-60-6595-3 (printed)
ISBN 978-952-60-6596-0 (pdf)
ISSN-L 1799-4934
ISSN 1799-4934 (printed)
ISSN 1799-4942 (pdf)
http://urn.fi/URN:ISBN:978-952-60-6596-0

Unigrafia Oy
Helsinki 2015

Finland

441 697
Printed matter

Aalto University

Abstract

Aalto University, P.O. Box 11000, FI-00076 Aalto www.aalto.fi

Author
Udesh Oruthota

Name of the doctoral dissertation
Performance Analysis and Mitigation Techniques for I/Q-Corrupted OFDM Systems

Publisher School of Electrical Engineering

Unit Department of Communications and Networking

Series Aalto University publication series DOCTORAL DISSERTATIONS 219/2015

Field of research Communications Engineering

Manuscript submitted 17 September 2015 **Date of the defence** 15 January 2016

Permission to publish granted (date) 12 November 2015 **Language** English

☐ **Monograph** ☒ **Article dissertation (summary + original articles)**

Abstract

Orthogonal Frequency Division Multiplexing (OFDM) has become a widely adopted modulation technique in modern communications systems due to its multipath resilience and low implementation complexity. The direct conversion architecture is a popular candidate for low-cost, low-power, fully integrated transceiver designs. One of the inevitable problems associated with analog signal processing in direct conversion involves the mismatches in the gain and phases of In-phase (I) and Quadrature-phase (Q) branches. Ideally, the I and Q branches of the quadrature mixer will have perfectly matched gains and are orthogonal in phase. Due to imperfect implementation of the electronics, so called I/Q imbalance emerges and creates interference between subcarriers which are symmetrically apart from the central subcarrier. With practical imbalance levels, basic transceivers fail to maintain the sufficient image rejection, which in turn can cause interference with the desired transmission. Such an I/Q distortion degrades the systems performance if left uncompensated.

Moreover, the coexistence of I/Q imbalance and other analog RF imperfections with digital baseband and higher layer functionalities such as multiantenna transmission and radio resource management, reduce the probability of successful transmission. Therefore, mitigation of I/Q imbalance is an essential substance in designing and implementing modern communications systems, while meeting required performance targets and quality of service. This thesis considers techniques to compensate and mitigate I/Q imbalance, when combined with channel estimation, multiantenna transmission, transmission power control, adaptive modulation and multiuser scheduling. The awareness of the quantitative relationship between transceiver parameters and system parameters is crucial in designing and dimensioning of modern communications systems. For this purpose, analytical models to evaluate the performance of an I/Q distorted system are considered.

Keywords I/Q imbalance, Performance analysis, Channel estimation, MIMO, Precoding, Link adaptation, D2D communication

ISBN (printed) 978-952-60-6595-3 **ISBN (pdf)** 978-952-60-6596-0

ISSN-L 1799-4934 **ISSN (printed)** 1799-4934 **ISSN (pdf)** 1799-4942

Location of publisher Helsinki **Location of printing** Helsinki **Year** 2015

Pages 139 **urn** http://urn.fi/URN:ISBN:978-952-60-6596-0

Preface

This doctoral thesis is based on a performance analysis of how Orthogonal Frequency Division Multiplexing systems suffer from I/Q distortion in their quadratic mixing and possible I/Q imbalance mitigation techniques. The research work for this doctoral thesis has been carried out at the Department of Communications and Networking (ComNet) of the School of Electrical Engineering, Aalto University. The work was funded by project Dirty-RF.

Firstly, I would like to express my deepest gratitude to my supervisor, Professor Olav Tirkkonen, for his constant guidance, support and inspiring collaboration, including numerous enlightening discussions that sometimes continued very late into the evening. It has been a great pleasure, honor and privilege, to work with him during my doctoral studies. I would also like to sincerely thank Dr. Nataliya Ermolova, who was an instructor for the initial stage of my research work, for her remarks and advice motivating me to succeed. Further, I would like to thank Dr. Prathapasinghe Dharmawansa for his valuable comments and support toward the success of my studies during his short stay.

My warm thanks also go to Dr. Michail Matthaiou, Queen's University, Belfast, United Kingdom, and Associate Professor Mats Bengtsson, KTH Royal Institute of Technology, Sweden, for their constructive comments while reviewing the manuscript of the thesis and which really improved the structure of the thesis.

I am grateful to the Department of ComNet for providing me with such an opportunity, and my special thanks go to my colleagues in the Department as well as in the research group, and the personnel of the Department, for a pleasant and inspiring working atmosphere. Mr. Victor Nias is also acknowledged for his contribution in making the research environment smooth and efficient.

Looking further back, I would like to express my gratitude to my beloved mother and my wife, who have been great sources of encouragement. Without their support and sacrifice, this work would never have been completed.

Otaniemi, December 4, 2015,

Contents

List of Publications

This thesis consists of an overview and of the following publications which are referred to in the text by their Roman numerals.

I U. Oruthota, O. Tirkkonen. SER/BER expression for M-QAM OFDM systems with imperfect channel estimation and I/Q imbalance. *EURASIP Journal on Wireless Communications and Networking*, 2012:303, September 2012.

II U. Oruthota, O. Tirkkonen, and N. Y. Ermolova. Analysis of space-frequency coded OFDM with I/Q imbalance. In *Proceedings of the International Congress on Ultra Modern Telecommunications and Control Systems, ICUMT*, pp. 275-280, October 2010.

III U. Oruthota, O. Tirkkonen. I/Q imbalance compensation in precoded MIMO-OFDMA systems. In *Proceedings of the International Symposium on Wireless Personal Multimedia Communications, WPMC*, pp. 291-295, September 2012.

IV U. Oruthota, O. Tirkkonen. Link adaptation of precoded MIMO-OFDMA system with I/Q interference. *IEEE Transactions on Communications*, vol. 63, no. 3, pp. 780-790, March 2015.

V U. Oruthota, O. Tirkkonen. I/Q interference in device-to-device underlay communication with uplink power control. In *Proceedings of the 81st IEEE Vehicular Technology Conference, VTC Spring*, pp. 1-5, May 2015.

Author's Contribution

Publication I: "SER/BER expression for M-QAM OFDM systems with imperfect channel estimation and I/Q imbalance"

The author has the main responsibility in writing this publication. The author has played a leading role in the theoretical modeling and planning of the work. The author has conducted a performance evaluation of the OFDM system in the presence of imperfect CSI and has built his own link-level simulator, as well as performed the system analysis presented in the publications.

Publication II: "Analysis of space-frequency coded OFDM with I/Q imbalance"

The author is the main contributor of this work, and has played a leading role in the theoretical modeling and planning of the publication. The author has conducted a performance evaluation of the SFBC-OFDM system and has built his own link-level simulator, as well as performed the system analysis presented in the publications.

Publication III: "I/Q imbalance compensation in precoded MIMO-OFDMA systems"

The author has the main responsibility in writing this publication and has played a leading role in the theoretical modeling and planning of the work. The author has conducted a performance evaluation of the precoded-MIMO-OFDM system and has built his own link-level simulator, as well as performed the system analysis presented here.

Publication IV: "Link adaptation of precoded MIMO-OFDMA system with I/Q interference"

The author has the main responsibility in writing this publication. The author has played a leading role in the theoretical modeling and planning of the work. The author has conducted a performance evaluation of the system and has built his own link-level simulator, as well as performed the system analysis presented in the publications.

Publication V: "I/Q interference in device-to-device underlay communication with uplink power control"

The author is the main contributor of this work, and has played a leading role in the theoretical modeling and planning of all publications. The author has conducted a performance evaluation of the systems in the presence of D2D transceivers and has built his own link-level simulator, as well as performed the system analysis presented in the publications.

List of abbreviations and symbols

Abbreviations

AMC	Adaptive Modulation and Coding
ARQ	Automatic Repeat Request
AWGN	Additive White Gaussian Noise
BER	Bit Error Rate
BLER	Block Error Rate
BPSK	Binary Phase Shift Key
CDF	Cumulative Distribution Function
CFO	Carrier Frequency Offset
CSI	Channel State Information
CQI	Channel Quality Indicator
DL	Downlink
FDD	Frequency Division Duplex
FFT	Fast Fourier Transform
FPC	Fractional Power Control
HARQ	Hybrid ARQ
ICI	Inter Carrier Interference
IFFT	Inverse Fast Fourier Transform
ILR	Image Leakage Ratio
IRR	Image Rejection Ratio
ISI	Inter-Symbol Interference
I/Q	In-phase/Quadrature phase
LMS	Least Mean Square
LTE	Long Term Evolution
MAC	Medium Access Control
MCI	Mirror Carrier Interference
MF	Matched Filter

MIMO	Multiple Input Multiple Output
MISO	Multiple Input Single Output
MLE	Maximum Likelihood Estimate
MMSE	Minimum Mean Square Error
MRC	Maximal Ratio Combining
MU	Multiuser
OFDM	Orthogonal Frequency Division Multiplexing
OFDMA	Orthogonal Frequency Division Multiple Access
PDF	Probability Density Function
QAM	Quadrature Amplitude Modulation
QoS	Quality of Service
RF	Radio Frequency
RLS	Recursive Least Square
RRM	Radio Resource Management
RV	Random Variable
SER	Symbol Error Rate
SFBC	Space Frequency Block Code
SINR	Signal-to-Interference plus Noise Ratio
SIR	Signal-to-Interference Ratio
SNR	Signal-to-Noise Ratio
STBC	Space Time Block Code
STC	Space Time Code
SVD	Singular Value Decomposition
TDD	Time Division Duplex
TPC	Transmit Power Control
UE	User Equipment
UL	Uplink

3GPP	3rd Generation Partnership Project

Symbols

C	Capacity of a system of interest
$\mathbb{C}$	Set of complex numbers
d	Distance between the base station and a user
$\mathbb{E}\{\cdot\}$	Expectation
f_c	Carrier frequency
$g_{R/T}$	Gain mismatch between I and Q branches of a receiver/transmitter
g_k	I/Q modulated channel coefficient on kth subcarrier
h_k	Channel frequency response on kth subcarrier
$\mathbf{H}, \tilde{\mathbf{H}}, \bar{\mathbf{H}}$	MIMO channel matrix
$\mathbf{I}$	Identity matrix
$\Im\{\cdot\}$	Imaginary part of a complex value
k_0	Path loss at cell edge (linear scale)
$K_{i,R/T}$	I/Q imbalance coefficients on the receiver/transmitter
L	Image leakage ratio
$M_{R/T}$	Number of receiver/transmitter antennas
n_k	AWGN sample on kth subcarrier
N	Number of active subcarriers in an OFDM system
N_0	Channel noise variance
P_0	Target received power
P_{max}	Maximum allowed transmit power of a mobile terminal
$\mathbf{R}$	Channel covariance matrix
$\Re\{\cdot\}$	Real part of a complex value
$\mathrm{Tr}\{\cdot\}$	Trace of a matrix
$\hat{x}$	Estimate of a given quantity x
$x_{LO}(t)$	Local oscillator output

γ	Instantaneous signal-to-interference ratio
γ_0	Average signal-to-noise ratio
ρ	Channel covariance
σ_x^2	Variance of x
$\phi_{R/T}$	Phase mismatch between I and Q branches of a receiver/transmitter

$(\cdot)^*$	Complex conjugate
$(\cdot)^H$	Hermitian transpose
$(\cdot)^T$	Transpose
$(\cdot)^{-1}$	Inverse
$\lvert\cdot\rvert$	Absolute value of a argument
$\lvert\lvert\cdot\rvert\rvert$	Euclidean norm of a vector

1. Introduction

1.1 Background

Growing requirements imposed upon communications transceivers have led to greater sensitivity to non-idealities in Radio Frequency (RF) front-end components. The traditional superheterodyne architecture is no longer the most attractive choice for the RF front-end due to its complicated structure. Instead, the simplest direct conversion architecture has become a widely adopted solution in low-cost, low-power, fully integrated transceiver design. One of the fundamental problems associated with analog signal processing in direct conversion involves the mismatches in the gain and phases of In-phase (I) and Quadrature-phase (Q) branches. Ideally, the I and Q branches of the quadrature mixer will have perfectly matched gains and be orthogonal during the phase. Due to the finite tolerance of practical electronics, so-called I/Q imbalance introduces mirror frequency interference and degrades performance if left uncompensated. The severity of the I/Q imbalance, then, can be quantified as the power of the mirror/image with respect to the desired frequency component. With practical imbalance levels, basic transceivers fail to maintain the sufficient rejection of the image frequency band, which in turn can cause interference with the desired transmission. Therefore, the elimination or mitigation of I/Q imbalance, while meeting stringent cost requirements, becomes a challenge in such communications systems. The goal of such compensation is to provide improved image frequency rejection, which by its nature depends on the accuracy of the estimation and compensation approach. Recent research efforts have dealt with the issue of I/Q imbalance, and have come up with different mitigation and compensation techniques in both the analog and digital domains [1, 2, 3]. In addition, fre-

quency response mismatch between the baseband digital-to-analog converters and low-pass filters of the I and Q branches introduces frequency-dependent I/Q mismatch, and as such compensation techniques have been studied in quite a number of papers [4, 5, 6, 7]

OFDM is gaining popularity as a modulation technique for current communications systems due to its multipath resilience and practical implementation complexity. The effect of I/Q imbalance is relatively significant in OFDM systems, since the mirror subcarriers which are symmetrically apart from the central subcarrier interfere each other. To eliminate the mirror carrier interference, various I/Q imbalance mitigation and compensation algorithms for OFDM have been proposed in the literature [5, 8, 9, 10].

Some existing I/Q imbalance estimation and compensation techniques are based on making use of pilot signals [11, 12]. However, the transmission of I/Q-immune pilots costs extra radio resources, and thus blind compensation methods are of great interest [13, 14, 15, 16, 17].

The combined effect of I/Q imbalance with other major RF impairments, such as phase noise, carrier frequency offset and non-linear distortion of power amplifiers, has been extensively studied. The effect of I/Q imbalance and phase noise on OFDM receivers have been investigated in [18, 19]. The estimation of I/Q imbalance parameters is often not reliable, even at a higher Signal-to-Noise Ratio (SNR) in the presence of power amplifier non-linear distortion. The combined effect of I/Q imbalance and power amplifier non-linearity has been addressed in [20, 21] and the references therein.

The I/Q imbalance has a dramatic effect on the performance of multi-antenna transmission where several parallel RF chains are needed. Interesting research studies can be found in [8, 9], where I/Q compensation techniques for Multiple Input Multiple Output (MIMO)-OFDM systems have been descried. Space Time Block Coding (STBC) is a well-known transmission technique that realizes diversity benefits in multi-antenna environments. I/Q imbalance mitigation in STBC-OFDM has been widely studied, and several techniques have been suggested in [22, 23]. To achieve spatial diversity in frequency selective fading channels with OFDM, Space Frequency Block coding (SFBC) can be utilized, whereby STBCs are used across different antennas in conjunction with subcarriers. Several I/Q imbalance compensation algorithms have been discussed in [24, 9], which suggest novel solutions for multiantenna systems

as well as for mobility environments. Transmit beamforming with receiver combining is another simple approach to achieving the full diversity of multiantenna transmissions [25, 26]. In [27], transmit antenna selection strategies are discussed for OFDM transmissions with transmitter I/Q imbalance, and both transmitter and receiver I/Q imbalance compensation have been discussed in [10].

Analytical models describing I/Q imbalance in OFDM transmission have recently been detailed in [28, 20, 29]. Furthermore, Krone and Fettweis-[30] carried out a capacity analysis for OFDM systems with transceiver I/Q imbalance. For multiantenna transceivers, analytical models have been proposed for Signal-to-Interference plus Noise Ratio (SINR), the Symbol Error Rate (SER) and capacity analysis [31, 32, 33]. The authors in [23] and [24] propose time-frequency domain I/Q imbalance compensation schemes. The authors in [34, 35] propose an analytical framework for STBC MIMO-OFDM to obtain the signal-to-interference and error probability at the output of the receiver.

The effect of I/Q imbalance can be extended to other communications topologies, such as relays and cognitive radio [36, 37]. An analytical model for OFDM link performance under various receiver impairments has been demonstrated in [38].

1.2 Scope of the thesis

It has been demonstrated that I/Q distortion degrades system performance dramatically, depending on the channel characteristics and the transmission topology used [5, 28, 38]. The quantitative relationship between transceiver parameters and system parameters is an essential factor in the design and implementation of a communications systems [20, 33]. As a consequence, the need for an analytical framework to evaluate the performance of a system is an important topic. Recently, OFDM has been extensively used in modern wireless communications as a robust modulation technique. This environment has opened up a research space to explore various I/Q imbalance mitigation and compensation techniques for OFDM systems. The analytical modeling and performance analysis for I/Q-distorted OFDM is thus an important research topic.

The majority of studies on I/Q-imbalance mitigation and compensation are made in the context of the baseband communications aspect of the physical layer of the radio link. In realistic cellular communications sys-

tems, I/Q interference interacts with multiple system functions, such as channel estimation and multiantenna transmission methods, as well as Medium Access Control (MAC) and Radio Resource Management (RRM) functionalities, such as Transmit Power Control (TPC), Adaptive Modulation and Coding (AMC) and scheduling. The coexistence of I/Q imbalance and other imperfections with these higher layer functionalities reduces the probability of successful transmission. Hence, the goal of this thesis is to analyze the performance of OFDM/Orthogonal Frequency Division Multiple Access (OFDMA) systems with possible I/Q imbalance compensation techniques, combined with the functionalities of channel estimation, multiantenna transmission, TPC, AMC and multiuser scheduling, which are essential in cellular communications systems.

1.3 Contributions and structure of the thesis

The surging interest in OFDM has resulted in research activities to make OFDM transceivers more reliable and cheaper. The direct conversion architecture has become a viable solution for such low-cost, low-power terminals. However, they suffer severely from RF impairments due to imperfect implementation of the electronics. I/Q imbalance is one of the unavoidable RF impairments which distort a desired transmission. This thesis highlights a few important transmission scenarios which boost the effect of I/Q imbalance at the receiver. The performance analysis discussed in the context presented is relevant to the selection of system design parameters. With careful analog design, $25 - 40$dB image attenuation can be achieved [39]. Here, numerical examples are considered with 25dB image attenuation throughout. The results discussed may be considered as performance bounds for a given transmission, which then yields requirements for network planning and optimization. The compensation techniques, and transmission and detection models proposed show improvements in the quality of the desired transmission from suppressing I/Q interference.

The contributions of the thesis lie in extending the detailed analysis of the performance of an I/Q-disturbed radio link to a receiver with imperfect channel estimation, and in designing novel SFBCs and joint precoding techniques for I/Q-distorted multiantenna channels. The thesis also embeds I/Q mitigation within a wider cellular system perspective. This is made explicit by detailed studies of I/Q-mediated near-far effects re-

lated to uplink TPC, as well as by link adaptation methods to mitigate I/Q interference in multiantenna systems.

This thesis is organized as follows. The introduction, scope of the study and its contribution are outlined in Chapter 1. Chapter 2 includes a detailed discussion of I/Q imbalance compensation, modeling and performance degradation due to I/Q imbalance. Chapter 3 studies channel estimation strategies and the estimation error model that is most commonly used. In Chapter 4, a comprehensive discussion of the impact of coding over I/Q imbalance is included. The MAC layer and RRM strategies employed in the I/Q imbalance domain are explained in Chapter 5. The conclusion is included in Chapter 6.

1.4 Summary of publications

This thesis consists of an introductory part and six original publications. The publications are listed on page vi and are appended at the end of the manuscript.

Comprehensive error probability analysis has been done in Publication I for Multiple Quadrature Amplitude Modulation (M-QAM) modulated I/Q-distorted OFDM transmission with imperfect channel estimation at the receiver. The proposed analytical framework highlights the non-Gaussian nature of receiver I/Q imbalance, which is especially visible for higher-order modulation. Further, it addresses the joint/separate estimation and equalization in imperfect channel estimation error situations. The closed form expressions for the symbol and bit error rate performances are derived for non-Gaussian I/Q interference. Here, Binary Phase Shift Key (BPSK) and Walsh-Hadamard based pilot structures are selected for separate and joint channel estimations, respectively.

The benefits of SFBC schemes under different fading characteristics are discussed with suitable compensation techniques in Publication II. Three SFBC structures are proposed and the post processing SINR is evaluated for Matched-Filter (MF) and Zero-Forcing (ZF) receivers with and without joint detection. The Alamouti code distribution across the mirror carriers offers free compensation of receiver I/Q imbalance in flat fading environments. When the channel becomes frequency selective, the performance tends to degrade due to I/Q induced non-orthogonality in the channel matrix.

In precoded OFDM/OFDMA, a precoder on a given subcarrier experi-

ences uncontrolled I/Q interference if there is a low-rank transmission on its mirror subcarrier. Hence, the separate selection of precoders on each subcarrier is no longer optimal; joint selection of precoders becomes essential. The joint optimization of mirror precoders in an MIMO-OFDMA system is discussed in Publication III. Gradient and line search algorithms are used to optimize precoders which are jointly selected to minimize the I/Q interference. Furthermore, an interference alignment method is studied for comparison. The gradient and line search algorithms perform better in the high SNR region and the interference alignment optimization follows a similar trend.

When precoders of the subcarriers are selected separately, mirror carrier interference due to a low-rank transmission may completely destroy the desired signal on the subcarrier of interest, resulting in poor SINR. Depending on the channel state information available at the transmitter, this may cause mispredictions of the channel quality, and accordingly losses of transmission. In such transmissions, link adaptation is discussed in Publication IV. Proper transmission methods can be selected based on knowledge of the SINR statistics in an I/Q aware link adaptation.

In an uplink cellular system, TPC is essential, and in Long Term Evolution (LTE), Fractional Power Control (FPC) is used. In [40], an analytical model for FPC in a cellular system is contributed. TPC causes variations in the interference level seen on the mirror subcarrier. This becomes an issue if cellular-controlled Device-to-Device (D2D) communications is used. An I/Q-mediated near-far effect emerges. In Publication V, this effect is discussed and analyzed based on the FPC analysis of [40].

2. I/Q Imbalance

The evolution of wireless communications systems has been driving the design and implementation of modern radio transceivers. The superheterodyne receiver is a widely used reception technique and finds numerous applications from personal communication devices to radio and TV tuners, and has been studied extensively in quite many papers. The use of the superheterodyne technique entails several trade-offs. Image rejection is a prevailing concern in this architecture. The IF must be sufficiently high so that the image channel lies in the stop-band of the RF pre-selection filter, otherwise the IF filter will pass this channel unattenuated in its own image passband. The fundamental difficulties with single-chip integration and high power consumption make alternative solutions appealing in many applications. The direct-conversion architecture has then become a popular candidate, and the need for the bulky off-chip filters and high power consumption is consequently removed by making it simple. However, direct conversion receivers are rather sensitive to RF impairments caused by the finite tolerance of electronic components. I/Q imbalance is the most notable impairment related to the direct-conversion architecture of an RF front-end that exploits analog quadrature mixing. It has been shown that the I/Q distortion complicates the design and dimensioning of communications networks [41, 20, 21, 42, 11],[30]-[32]. In order to cope with this impairment, different compensation techniques have been proposed.

OFDM has been widely employed in modern wireless networks as a robust modulation technique. OFDM is also sensitive to non-idealities in the RF front-ends, and I/Q imbalance has been identified as a key front-end effect. The I/Q imbalance results in Inter-Carrier Interference (ICI) from the mirror carrier of the OFDM symbol. The resulting distortion can limit the achievable data rate, and hence the performance of the system.

The resulting I/Q imbalance can be split into a frequency-flat and a frequency-selective part. The gain and phase mismatch occurs between the local oscillator signals used for up/down-conversion of the I and Q signals leads to a frequency-flat I/Q imbalance, and are being constant for all subcarriers in OFDM. The frequency-selective I/Q imbalance is mainly caused by mismatch between the filters in the I and Q path, and is dominated by the low-pass filters. For the consistency, we will focus on frequency-flat I/Q imbalance here after, and the frequency-selective case is left.

2.1 An I/Q Imbalance Model

The direct-conversion architecture is widely used in low-cost, low-power transceivers in modern wireless systems. However, the quadrature modulator and demodulator in the direct conversion architecture are sensitive to non-idealities of the electronic components in the I and Q branches which cause I/Q imbalance. As a result, there is a leakage of interference between the I and Q branches which adversely affects the performance of wireless systems. Both transmitter and receiver I/Q imbalance are pertinent to the direct conversion architecture. It has been shown that the major contribution is made by receiver I/Q imbalance [11].

Let us concentrate on a basic quadrature demodulator of the direct conversion receiver. Ideally, the gains of the I and Q branches of the demodulator are equal and orthogonal while in phase. However, in practice a substantial amount of gain and phase mismatch are visible in an imbalanced local oscillator, which leads to frequency-flat I/Q imbalance. This is modeled by effective gain g_R and phase ϕ_R imbalances at the receiver. The carrier waveform of the local oscillator can be represented by

$$x_{LO}(t) = \cos(2\pi f_c t) - j g_R \sin(2\pi f_c t + \phi_R) \tag{2.1}$$

with the corresponding carrier frequency f_c. The equivalent complex domain signal is thus

$$x_{LO}(t) = K_{1,R} e^{-j2\pi f_c t} + K_{2,R} e^{j2\pi f_c t} \quad , \tag{2.2}$$

where $K_{1,R} = (1 + g_R e^{-j\phi_R})/2, \quad K_{2,R} = (1 - g_R e^{j\phi_R})/2$ are the frequency-flat complex I/Q imbalance coefficients. Let us assume $r(t)$ to be the interference free baseband equivalent signal. As such, the received signal is $\tilde{r}(t) = 2\Re\{r(t)e^{j2\pi f_c t}\}$. The output of the quadrature mixer can be drawn

from $y(t) = \mathrm{LPF}\{\tilde{r}(t) \cdot x_{LO}(t)\}$, where $\mathrm{LPF}\{u(t)\}$ denotes the low-pass filtering process of the signal $u(t)$. Ultimately, the output baseband received signal becomes

$$y(t) = K_{1,R} r(t) + K_{2,R} r^*(t) \ . \tag{2.3}$$

Hence, in direct conversion receivers, the impact of I/Q mismatch can be viewed as a self-image problem, where the baseband equivalent signal is interfered with by its own complex conjugate. Likewise, at the transmitter, the carrier waveform of an imbalanced local oscillator can be represented as $x_{LO}(t) = \cos(2\pi f_c t) + j g_T \sin(2\pi f_c t + \phi_T)$. Therefore, a similar self-image interpretation can also be established on the transmitter side, and the output of the transmitter after I/Q corruption is

$$s(t) = K_{1,T} x(t) + K_{2,T}^* x^*(t) \ . \tag{2.4}$$

The ideal baseband equivalent transmitted signal under perfect matching is $x(t)$, and the frequency-flat I/Q imbalance coefficients of the transmitter are given by $K_{1,T} = (1 + g_T e^{j\phi_T})/2$ and $K_{2,T} = (1 - g_T e^{-j\phi_T})/2$.

With perfect matching, $g = 1$ and $\phi = 0$, and thus $K_1 = 1$ and $K_2 = 0$ for both transmitter and receiver. The severity of the I/Q imbalance can be characterized by the Image Rejection Ratio(IRR), $|K_1/K_2|^2$. The Image Leakage Ratio (ILR), L (the inverse of the IRR), is another parameter used to measure I/Q imbalance [31]. In the current RF-analog technology, a gain imbalance g of $1 - 2\%$ and a phase imbalance ϕ of $1 - 2^\circ$ may be expected, resulting in $25 - 40$ dB of image rejection [39].

Considering (2.4), the frequency domain equivalent model for the frequency-flat I/Q distortion at the receiver would be

$$y(f) = K_{1,R} r(f) + K_{2,R} r^*(-f) \ , \tag{2.5}$$

where $r(t) \rightarrow r(f)$ and $y(t) \rightarrow y(f)$ are the Fourier transform pairs. As a consequence, the effect of I/Q imbalance can be interpreted as an ICI between mirror frequency components [9, 42, 43].

In OFDM systems, a block of data is transmitted as an OFDM symbol. Assuming a symbol size equal to N (where N is a power of 2), the transmitted block of data is denoted by $\mathbf{z} = [z_1, .., z_k, .., z_N]^T$ where $[\cdot]^T$ is the transposition operation. The symbols on subcarrier k and its mirror $-k$ before being distorted by I/Q imbalance are z_k and z_{-k} (represented alternatively by z_{N-k+2}), respectively. Without any change in their indices, the samples on subcarrier and its mirror are the same for $k = 1, N/2 + 1$. For all other subcarriers, their indices become mirrored around the $k = N/2 + 1$. In order to have a unified formulation for all the subcarriers, these two tones

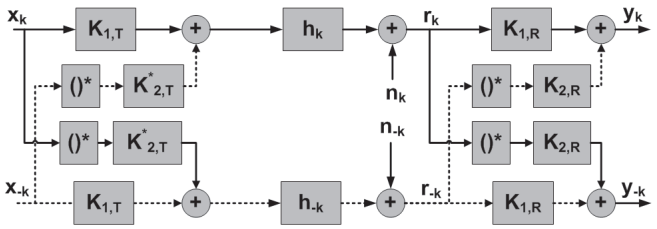

Figure 2.1. A basic transmission model with transmitter and receiver I/Q imbalance.

are discarded. From the frequency domain translation (2.5), the received symbol on subcarrier k is given by

$$y_k = K_{1,R} z_k + K_{2,R} z^*_{-k}, \quad k = 1, .., N/2 - 1, \quad k \neq 1, N/2 + 1 \ . \tag{2.6}$$

The effect of fading and channel noise are omitted here. The symbol on subcarrier k is interfered with by the transmission on its mirror subcarrier, and vice versa. The induced ICI can be specifically identified as mirror carrier interference [9, 43]. More precisely, the effect of the transmitter and receiver I/Q imbalance on the mirror subcarrier pair are depicted in Figure 2.1. The complex channel coefficients on the subcarrier and its mirror are denoted by h_k and h_{-k}, respectively. Similarly, the Additive White Gaussian Noise (AWGN) samples on the mirror carrier pair are defined by n_k and n_{-k}. The I/Q distortion-free transmitted symbols on the mirror subcarrier pair are x_k and x_{-k}, and the received symbols after I/Q distortion are represented by y_k and y_{-k}. In the presence of channel fading and noise, the ultimate received signal on subcarrier k with the transmitter and receiver I/Q distortion is

$$y_k = g_k x_k + g_{-k} x^*_{-k} + K_{1,R} n_k + K_{2,R} n^*_{-k} \ , \tag{2.7}$$

where g_k and g_{-k} are the I/Q modulated channel frequency responses on the subcarrier and its mirror (Refer Figure 2.1)

$$g_k = K_{1,R} h_k K_{1,T} + K_{2,R} h^*_{-k} K^*_{2,T}$$
$$g_{-k} = K_{1,R} h_k K^*_{2,T} + K_{2,R} h^*_{-k} K^*_{1,T}$$

The signal model in (2.7) can be extended to a multiantenna system with M_T transmit antennas and M_R receive antennas [5, 44]. The $M_R \times 1$ received signal vector on the subcarrier k is thus

$$\mathbf{y}_k = \mathbf{G}_k \mathbf{x}_k + \mathbf{G}_{-k} \mathbf{x}^*_{-k} + \mathbf{K}_{1,R} \mathbf{n}_k + \mathbf{K}_{2,R} \mathbf{n}^*_{-k}. \tag{2.8}$$

The $M_R \times M_T$ I/Q modulated channel matrix on subcarrier k is defined by $\mathbf{G}_k = \left(\mathbf{K}_{1,R}\mathbf{H}_k\mathbf{K}_{1,T} + \mathbf{K}_{2,R}\mathbf{H}^*_{-k}\mathbf{K}^*_{2,T}\right)$ and the corresponding channel matrix on the mirror carrier is $\mathbf{G}_{-k} = \left(\mathbf{K}_{1,R}\mathbf{H}_k\mathbf{K}^*_{2,T} + \mathbf{K}_{2,R}\mathbf{H}^*_{-k}\mathbf{K}^*_{1,T}\right)$. The $M_T \times 1$ vector $\mathbf{x}_k$ contains transmit symbols on each antenna on the subcarrier and the symbol vector x_{-k} on the mirror. The effects of transmitter and receiver I/Q imbalance are characterized by the $M_T \times M_T$ matrices $\mathbf{K}_{1,T} = \left(\mathbf{I} + \mathbf{g}_T e^{j\phi_T}\right)/2$ and $\mathbf{K}_{2,T} = \mathbf{I} - \mathbf{K}^*_{1,T}$, as well as the $M_R \times M_R$ matrices $\mathbf{K}_{1,R} = \left(\mathbf{I} + \mathbf{g}_R e^{-j\phi_R}\right)/2$ and $\mathbf{K}_{2,R} = \mathbf{I} - \mathbf{K}_{1,R}$. Here, $\mathbf{g}$ and ϕ are the diagonal matrices with the gain and phase mismatches on each transmitter/receiver branch.

Within a practical range of IRR values [39], and without loss of generality, we can approximate the I/Q imbalance coefficients by $K_{1,T/R} \approx 1$ and $K_{2,T/R} \approx \epsilon_{T/R}$, where ϵ is a small complex quantity. As $\epsilon_R\epsilon_T << 1$, an implicit second-order I/Q interference term in (2.8) can be omitted, resulting in a signal model Publication III,Publication IV,

$$\mathbf{y} \approx \mathbf{H}_k\mathbf{x}_k + \left(\mathbf{E}_R\mathbf{H}^*_{-k} + \mathbf{H}_k\mathbf{E}^*_T\right)\mathbf{x}^*_{-k} + \mathbf{n}_k + \mathbf{E}_R\mathbf{n}^*_{-k}\,, \tag{2.9}$$

where $\mathbf{E}_{T/R}$ is a diagonal matrix which contains the image attenuations $\epsilon_{T/R}$ of each transmission chain. The above MIMO-OFDM model decouples the effect of transmitter and receiver I/Q imbalance, and the mathematical manipulation is thus rather simple. When considering an OFDMA system where there are multiple users scheduled on different frequency resources, one can obtain a similar signal model and thus the I/Q interference comes from both channels, $\mathbf{H}_k$ and $\mathbf{H}_{-k}$, which are allocated for the users on a subcarrier and its mirror, respectively.

2.2 Performance Degradation

As stated earlier, the low-cost implementation of quadratic conversion suffers from gain and phase imbalance, which causes cross-talk between mirror signals and degrades the system performance of a system [9, 43]. The IRR or ILR quantifies the suppression of the image signal and usually lies within the range of $25 - 40$dB [39]. The quantitative analysis of performance then becomes a key factor in the design and optimization of such a communications network. For simplicity, frequency-flat receiver I/Q imbalance is chosen for the analysis.

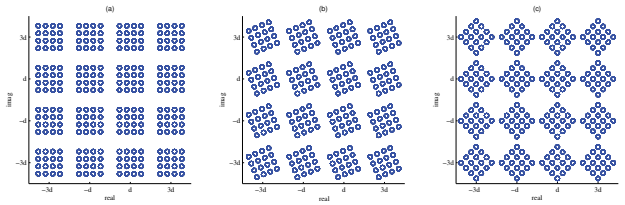

Figure 2.2. Received 16-QAM constellations for different phases of the complex-valued leakage ratio L_k and a fixed magnitude of $|L_k| = -25$dB: a) $\angle L_k = 0$, b) $\angle L_k = \pi/8$ and c) $\angle L_k = \pi/4$.

2.2.1 Constellation Rotation

In this section, we demonstrate the constellation rotation caused by the I/Q imbalance. For simplicity of the presentation, the receiver I/Q imbalance effect is considered. From (2.7) by letting $K_{1,T} \to 1$ and $K_{2,T} \to 0$, we get

$$y_k = K_{1,R} h_k x_k + K_{2,R} h^*_{-k} x^*_{-k} + K_{1,R} n_k + K_{2,R} n^*_{-k}. \tag{2.10}$$

The estimated transmit symbol on subcarrier k can then be computed from

$$\hat{x}_k = x_k + \frac{K_{2,R}}{K_{1,R}} \frac{h^*_{-k}}{h_k} x^*_{-k} + \frac{K_{1,R} n_k + K_{2,R} n^*_{-k}}{K_{1,R} h_k}. \tag{2.11}$$

The image attenuation with regard to the desired channel is denoted by $l_k = \frac{K_{2,R}}{K_{1,R}}$. The symbol estimate of x_k in (2.11) is thus

$$\hat{x}_k = x_k + l_k \frac{h^*_{-k}}{h_k} x^*_{-k} + \frac{n_k}{h_k} + l_k \frac{n^*_{-k}}{h_k}. \tag{2.12}$$

Each symbol on the mirror subcarrier is multiplied by l_k (ILR, $L_k = |l_k|^2$) so that the mirror constellation is rotated with respect to the original constellation. In order to illustrate this effect, an exemplary 16-QAM constellation is shown in Figure 2.2 for $\mathrm{ILR} = -25$dB with different $\angle L_k$. It is clear that taking amplitude distortion into account is not sufficient. The phase rotation due to I/Q imbalance is also a key factor [28] that needs to be considered in relation to reception and performance analysis.

2.2.2 Effect of the Channel

From (2.12), the total distortion of a received signal due to I/Q imbalance, fading and channel noise can be characterized by the displacement vector

$$\Delta_k = l_k \frac{h^*_{-k}}{h_k} x^*_{-k} + \frac{n_k}{h_k} + l_k \frac{n^*_{-k}}{h_k} \quad . \tag{2.13}$$

The statistics of the displacement vector Δ_k depend on the channel coefficients on the carrier of interest $h_k,\ h_{-k}$ as well as the AWGN noise

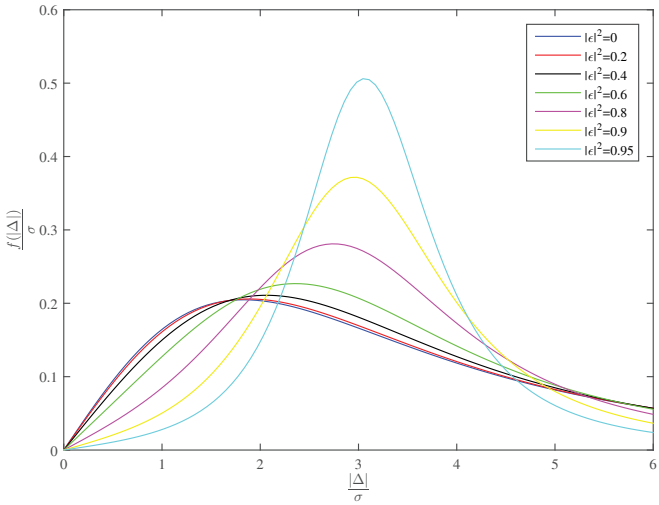

Figure 2.3. PDF of the magnitude of the error displacement vector $f_\Delta(|\Delta_k|)$.

samples $n_k,\ n_{-k}$. Note that the noise after I/Q corruption becomes spatially colored. It is important to notice that the channel coefficients may, in general, be correlated. The correlation between the pair of channel coefficients h_k and h_{-k} is described by the complex-valued covariance $\rho_k = \mathbb{E}\{h_k h_{-k}^*\}$. In practical communications systems, the coherence bandwidth is smaller than the system bandwidth, and thus the mirror carrier pairs can often be assumed to be uncorrelated [28, 31, 34].

For performance analysis, we may consider a distribution of the channels h_k and h_{-k}. Combined with the distribution of the i.i.d AWGN samples n_k and n_{-k}, we may derive the distribution of the displacement vector in closed form [28]. Figure 2.3 describes the behavior of the magnitude distribution function $f_\Delta(|\Delta_k|)$ for different values of the correlation ρ_k. The displacement can be modeled as a quotient of two complex Gaussian Random Variables (RVs), and the variances is $\sigma^2 = L_k|x_{-k}|^2 + (1+L_k)\frac{N_0}{\sigma_h^2}$ where σ_h^2 and N_0 denote the variance of the channel h and the noise. The squared magnitude of the correlation between them is $|\epsilon|^2 = \left|\frac{\rho_k}{\sigma_h^2}\right|^2 \frac{L_k|x_{-k}|^2}{\sigma^2}$ and the channel correlation ρ_k is hidden inside. The distribution of the displacement becomes more Gaussian when the channels tend to be uncorrelated and it exhibits a dispersion with the increasing effect of correlation.

Figure 2.4 shows the SER performance when the mirror channels are completely uncorrelated in a Rayleigh fading environment. Note the significant error-floors due to the I/Q imbalance, which can be observed even

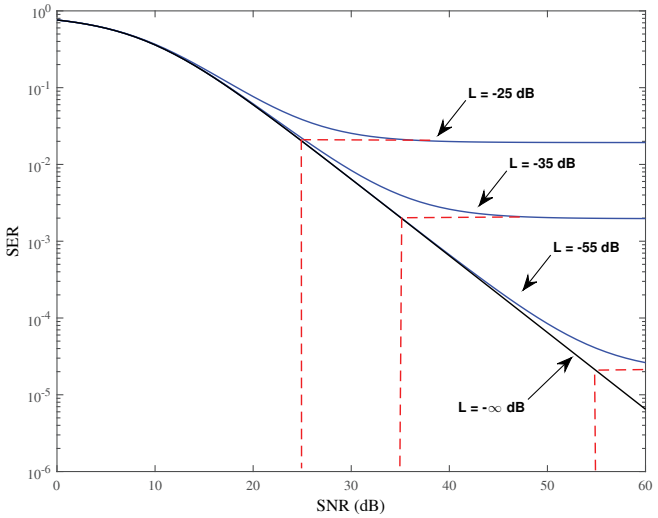

Figure 2.4. SER performance vs SNR of the receiver I/Q imbalance-corrupted system in a Rayleigh fading environment for different ILR levels.

for ambitious IRR values of 50dB and above. The asymptotic Signal-to-Interference Ratio (SIR) can be predicted by projecting the asymptotic error floor onto the ideal receiver's performance. It is almost equal to the IRR Publication I. Furthermore, the performance shown in the figure can be argued as the SER upper bound for a system suffering from receiver I/Q imbalance.

2.2.3 Capacity

The maximum theoretical data rate that a communications system can provide for reliable transmission is defined by its capacity [45]. When the channel is fading, one has to distinguish between ergodic capacity and outage capacity [46]. OFDM systems appear to be quite sensitive to I/Q imbalance and system capacity is reduced. From (2.10), the corruption due receiver I/Q interference can be characterized by the average SINR, and it can be stated for a given channel realization as in [30],

$$\bar{\gamma}_k = \frac{\mathbb{E}\{|K_{1,R} h_k x_k|^2\}}{\mathbb{E}\{|K_{2,R} h^*_{-k} x^*_{-k} + K_{1,R} n_k + K_{2,R} n^*_{-k}|^2\}} \,. \tag{2.14}$$

The random variables x_k, x_{-k}, n_k and n_{-k} can be assumed to be independent of each other, and the statistical averages $\mathbb{E}\{\cdot\}$ are computed accordingly. In addition, it is reasonable to assume that x_k and n_k of the individual subcarriers are identically distributed with zero means and variances, $\sigma_x^2 = \mathbb{E}\{|x_k|^2\}$ and N_0, respectively. With these assumptions, the average

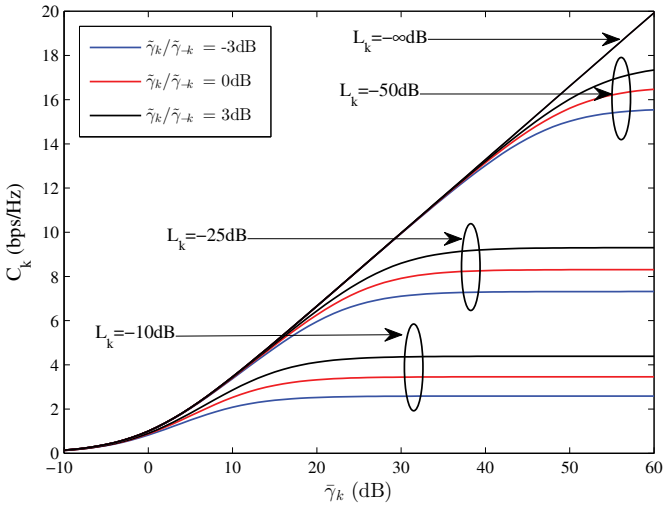

Figure 2.5. Impact of receiver I/Q imbalance on the system capacity C_k for different L_k and fixed channel realizations, $\tilde{\gamma}_k/\tilde{\gamma}_{-k}$.

SINR becomes

$$\bar{\gamma}_k = \frac{\tilde{\gamma}_k}{1 + L_k(1 + \tilde{\gamma}_{-k})} \quad , \tag{2.15}$$

where $\tilde{\gamma}_k = |h_k|^2 \frac{\sigma_x^2}{N_0}$ is the SNR of the ideal receiver without I/Q distortion. Similarly, the average SNR of the mirror subcarrier $\tilde{\gamma}_{-k}$ can be defined. OFDM transforms a frequency selective channel into a set of frequency flat parallel channels, which in terms of capacity boils down to an AWGN channel for each subcarrier [46]. Accordingly, the capacity of one subcarrier for a fixed channel realization would be

$$C_k = \log_2\left(1 + \frac{\tilde{\gamma}_k}{1 + L_k(1 + \tilde{\gamma}_{-k})}\right) \quad . \tag{2.16}$$

In Figure 2.5, one can observe how the receiver I/Q imbalance affects the system capacity for a fixed channel realization. The system capacity C_k shows a strong correlation with L_k as well as with the SNR ratio $\tilde{\gamma}_k/\tilde{\gamma}_{-k}$. For a given L_k, the system capacity decreases if $\tilde{\gamma}_k$ becomes less than $\tilde{\gamma}_{-k}$. The lower and upper asymptotes of C_k that are apparent from Figure 2.5 can be derived analytically by considering the two cases of very high and vanishing noise variance σ_n^2.

Considering the whole set of subcarriers that are available for data transmission, the overall system capacity is the sum of the capacities of the individual subcarriers, and for fading channels it is sufficient to concentrate on a single subcarrier for the analysis. The channel coefficient h_k can be represented in terms of the polar form, $|h_k| = a_k$, where the

absolute value $a_k \in (0,\ \infty)$, the ergodic capacity for the kth subcarrier, is now given by

$$\bar{C}_k = \int_0^\infty \int_0^\infty \log_2 \left(1 + \frac{a_k^2 \frac{\sigma_x^2}{N_0}}{1 + K_k \left(1 + a_{-k}^2 \frac{\sigma_x^2}{N_0} \right)} \right) f(a_k, a_{-k}) da_k da_{-k} \ . \quad (2.17)$$

For a given joint channel amplitude distribution $f(a_k, a_{-k})$, the capacity of the system can be derived as in [47]. The joint effect of transmitter and receiver I/Q imbalance has been addressed in [30]. In parallel, the ergodic capacity for a Multiple Input Single Output (MISO) system with both transmitter and receiver I/Q imbalance is discussed in [48], further extending the result in to MIMO transmission in Publication IV.

2.3 I/Q Imbalance Mitigation

I/Q imbalance degrades the effective SINR and causes performance degradation. The impact of I/Q imbalance is more severe for systems employing high-order modulations and high coding rates. Therefore, effective I/Q imbalance compensation is essential in the design of high data-rate systems employing the direct conversion architecture.

Digital signal processing has been considered to some extent as an effective I/Q compensation strategy [12, 49, 50]. Generally speaking, the common approach is to estimate the mismatch parameters using training data and then use these estimates in a simple digital re-matching network. This approach with time domain processing is considered in [49, 50]. The techniques in [12] use the mismatch estimates in the frequency domain to cancel the corresponding I/Q-induced ICI.

The Least Mean Square (LMS) algorithm has been implemented in direct conversion receivers for smooth adaptation [12, 11], and applications on low-IF receivers can be found in [51]. As the LMS algorithm is typically slow and the steady-state performance exhibits high variance due to the stochastic nature of the LMS algorithm, this makes it less attractive for high-speed applications, and thus authors in [52, 53] propose Maximum-Likelihood (ML) and Least-Squares (LS) estimation [52, 54] based approaches to compensate for I/Q imbalance. In [33], I/Q imbalance compensation in multiantenna systems were discussed. The ML estimate based method works well at a low SNR while the LS estimate outperforms it at a high SNR.

Several adaptive filtering schemes were proposed to eliminate the dis-

tortion of both frequency-flat and frequency-selective I/Q imbalances for OFDM systems. The adaptive I/Q canceler in the baseband domain has been introduced in [55]. An alternate adaptive structure operating on the frequency-domain samples can be found in [12]. Furthermore, symmetric adaptive decorrelation which for OFDM becomes a two-tap equalizer in the frequency domain can be used for image rejection [11, 56], which offers relatively high compensation accuracy. A Kalman filter based I/Q compensation approach which demonstrates good ability in tracking the channel time variations with a fast convergence speed has been demonstrated in [54].

Many compensation techniques rely on known pilot data or else known signal structures such as known data modulation or constellation. This type of method has been proposed recently in [18, 11, 57, 58, 59, 60], where I/Q compensation in OFDM modulation with known pilot data is considered. Blind compensation approaches work without specifically designed pilot structures. In [14, 15, 61, 62], blind signal estimation strategies are used to tackle I/Q imbalance at the receiver. For both transmitter and receiver I/Q imbalance, compensation in MIMO-OFDM has been suggested in [8]. Furthermore, I/Q imbalance compensation can be performed for STBC-MIMO to preserve diversity gains, as discussed in [23, 22].

It has been demonstrated that the circularity of the received complex signal is generally lost due to I/Q imbalance, and thus the compensation can be established using the statistical properties of the received signal, as in [13, 16, 17]. An identical approach can be found in [63] and [61] for frequency-selective I/Q imbalance as well. In parallel, an adaptive I/Q decorrelation based compensation scheme has been proposed in [14].

Several methods have recently been proposed for compensating I/Q imbalance in OFDM transmitters [64, 65, 66, 4]. In [64], a time-domain approach is presented which compensates for frequency-selective I/Q imbalance using an online operation. An approach in [66] makes use of a specialized calibration signal and offline calibration. Keith *et al.* [65] came up with a frequency domain online adaptive pre-distortion scheme to overcome the frequency-dependent I/Q imbalance at the transmitter while reducing computational complexity. A simple frequency-domain compensation structure is derived based on a traditional adaptive interference canceler in [67, 4]. Further, frequency selective I/Q imbalance can be efficiently compensated by decomposing the spectrum of the input signal to frequency-flat cases [15].

3. I/Q Imbalance with Imperfect Channel Estimation

3.1 Background

Channel State Information (CSI) is crucial for data detection and channel equalization. The role of CSI is further accentuated in multiantenna transmissions, by which significant improvements in capacity can be achieved through the use of transmitter and receiver diversity [68, 69]. However, the gains of such systems rely upon the knowledge of CSI at the receiver.

In practical systems, CSI can be achieved basically in two different ways: one is based on training symbols that are *a priori* known at the receiver while the other is blind, i.e., it relies only on the received symbols and acquires CSI by exploiting statistical information and/or transmitted symbol properties [70, 71]. Compared with training, blind estimation generally requires a long data record. Hence, it is limited to slowly time-varying channels and entails high complexity. Therefore, training-based channel estimation is a commonly used technique in the design and implementation of communications systems. Typical procedures for identifying the channel based on training utilize multiple OFDM symbols that completely consist of pilot symbols. Extending this idea to MIMO-OFDM systems is not straightforward, since not only the placement of the pilot tones but also the pilot sequences themselves must be optimized. The location, number and power of the pilot symbols embedded in multicarrier transmissions over fading channels are important design parameters affecting not only channel estimation performance but also channel capacity. It is shown that the optimal pilots in terms of sequences minimizing the mean-square channel estimation error have to be equipowered, equispaced, and orthogonal while in phase [72, 73, 74].

In such systems, the CSI is estimated prior to any reception of data. When the CSI changes significantly, a retraining sequence is transmitted. In a fast time-varying environment, such systems must continuously retrain in order to re-estimate the CSI. Between retraining sessions, these systems experience an increased Bit Error Rate (BER) due to their outdated channel estimates [73].

The structure of the OFDM signaling allows a channel estimator to use both time and frequency correlation. Such a two-dimensional estimator structure is generally too complex for a practical implementation, and reduced complexity solutions are proposed in [75, 76].

I/Q mitigation techniques can be implemented both in analog and digital domains [12, 49, 50]. In these, perfect CSI has been assumed. However, in a practical radio communications system, the actual channel quantities are I/Q-modulated and the I/Q imbalance and channel equalization are strongly interdependent. Therefore, the I/Q mismatch should be taken into account in equalizer design, particularly with high-order symbol alphabets [1]. In practical systems, errors in the channel estimation stage may result in excessive errors at the equalizer output [77, 38]. This problem has been addressed well in Publication I. The subsequent sections outline the training-based and blind estimation-based techniques commonly used in communications for both the channel and I/Q imbalance estimations.

3.1.1 Training-based Channel Estimation

The pilots and/or preambles are fundamental building blocks in many practical OFDM wireless systems. The existence of reference symbols is essential for the channel estimation as well as synchronization in time and frequency. The accuracy of the I/Q imbalance parameter estimation can be significantly increased if the pilot symbols are properly arranged.

Existing pilot designs for OFDM [73, 78] experience non-optimal estimation performance when I/Q imbalance exists. Frequency domain estimation and compensation was proposed in [79, 80, 60], where the receiver I/Q imbalance present on the channel estimate is canceled out by an asymmetric pilot allocation. Here, the interference from the opposite sideband is random and crosstalk can be removed by considering enough averaging either in time or in frequency. Meanwhile, in [58], the authors proposed a pilot design criterion in order to minimize the I/Q imbalance estimation MSE in OFDM transceivers.

In [11, 81], the authors propose a joint channel and distortion estimation technique requiring a large number of training symbols. The estimator utilizes a special pilot pattern to effectively estimate channel and I/Q imbalance by inserting null tones in the training symbols. Thus, the received training symbols are not affected by mutual interference between pairs of symmetric subcarriers. Even though the I/Q imbalance is efficiently estimated and compensated for, zero subcarriers should be avoided from the channel estimation point of view. A complementary subset of pilots described in [81], avoiding the need for null tones, ensures greater robustness against strongly frequency-selective fading channels.

In [50, 18, 82], the authors estimate I/Q imbalance from differences of estimated modulated channels at neighboring subcarriers, when the adjacent subcarrier channels are strongly correlated and I/Q imbalance is low and frequency flat. Standard pilots defined by IEEE 802.11g [83] are used. Based on the assumption that the I/Q imbalance parameters do not have sharp transitions and vary smoothly over a given amount of successive subcarriers, the authors in [7] proposed an iterative algorithm.

Different RF chains of MIMO branches can cause different I/Q imbalance levels, which further complicate channel estimation, since interference among multiple antennas needs to be avoided [84]. A pilot design for MIMO-OFDM systems with transceiver I/Q imbalance was proposed in [5], where it uses two OFDM symbols as a basic block which is repeated according to Walsh-Hadamard sequences for multiple antennas, a MIMO extension of what was proposed for SISO in [79]. It is overhead inefficient as a full preamble is used for training. An overhead efficient, white-noise optimal pilot designs for estimation of the equivalent channel responses incorporating both frequency flat and selective transceiver I/Q imbalances has been proposed in [59]. In [9], the authors develop comb-type pilot structure to jointly mitigate the ICI induced due to both I/Q imbalance and mobility.

A priori known BPSK symbols are chosen as set of orthogonal pilots to estimate the gain and phase errors in I/Q corrupted OFDM systems [79, 80, 60]. It uses an even number of OFDM training symbols with non-zero pilots where the pilots at the positive (negative) subcarrier indexes of the even symbols are the same as (negatives of) the corresponding pilots at the odd training symbols. Such pilot allocation can be easily extended to MIMO using Walsh-Hadamard sequence [5], where it creates orthogonality between mirror subcarrier pairs and between the different transmitter

branches.

In [85] constant amplitude, zero auto-correlation and Pseudorandom number sequences are proposed as training sequences. The pilot design criterion in [58] is derived in order to minimize the I/Q imbalance estimation MSE. In a practical situation, carefully chosen pilots [58, 86] should be set in order minimize the PAPR as well.

3.1.2 Non Data-aided (Blind) Estimation

A blind estimation technique has been discussed in [87] based on the assumption of uncorrelated transmitted subcarriers. In order to determine the I/Q imbalance coefficients, cross-correlation and the power of the sum of the imbalanced symbols on mirror carrier pairs were evaluated. This method needs a high number of received data symbols for a good statistical estimation of the I/Q imbalance. If the number of data symbols is not sufficient, an error floor occurs even for a high SNR region. Further enhancements of the blind estimator can be achieved through the application of Kalman filtering, including tracking and compensation of time-varying and frequency-selective I/Q imbalance [88].

A blind signal estimation scheme proposed in [14] for the conjugate signal model - where the observed signal is a linear combination of the desired signal and its complex conjugate - can be applied to the I/Q distorted systems - a one practical application where the image signal interference causes attenuation on the desired signal. Blind signal recovery is feasible when the second-order statistics of the observed signal. The circularity of the received signal is generally lost due to I/Q imbalances, and thus the compensation can be performed by projecting the received signal back to the "circular domain" [16, 17, 13] in OFDM systems. In [1] similar approach can be found for both transmitter and receiver I/Q imbalance compensation. In addition to the computational complexity, this property limits the application of this technique for OFDM applications as the number of subcarriers and the modulation order become larger.

3.2 Least Square Channel Estimation

High spectral efficiency is provided by M-QAM, which is widely employed in wireless communications applications [89, 90]. Performance analysis of M-QAM receivers is important in understanding the limitations on

high spectral efficiency communications and in designing adaptive modulation schemes [91]. In practice, the channel estimates cannot be perfect in fading channels and the adverse effect of imperfect channel estimation must be considered for accurate performance evaluation. Assuming perfect CSI, the performance of an OFDM system with a receiver I/Q imbalance is studied in [28] for different channel scenarios. The error rate performance for OFDM direct conversion receivers with synchronization and channel estimation imperfections has been addressed in [38] and an extension to STBC was proposed in [35].

Here, we consider an OFDM system where the reception is disturbed by transmitter and receiver I/Q imbalance. The information is M-QAM modulated to different OFDM data subcarriers and then transformed to a time domain signal by the Inverse Fast Fourier Transform (IFFT) operation and prepended by a cyclic prefix, which is chosen to be longer than the maximal channel impulse response. The I/Q corrupted discrete complex baseband signal for the kth subcarrier after the receiver FFT processing is given by (2.7). In broadband communications, it is a realistic assumption that the channel coherence bandwidth is smaller than the typical frequency separation between a mirror carrier pair. Hence, without loss of generality, we can assume that there are frequency selective channels with independently fading mirror carriers.

The estimate of the modulated channel h is denoted by $\hat{h}$. For i.i.d. signal branches, $\mathbb{E}\{|\hat{h}|^2\} = \sigma_{\hat{h}}^2$ is assumed for all k. Let the normalized correlation coefficient between $\hat{h}$ and h be defined as $\rho = \mathbb{E}\{\hat{h}^* h\}/\sigma_h \sigma_{\hat{h}}$, where σ_h and $\sigma_{\hat{h}}$ are the standard deviations of the channel h and its estimate $\hat{h}$, respectively. The channel estimation error at the kth subcarrier is given by $e = \hat{h} - h$. For Minimum Mean Square Error (MMSE) channel estimation $\mathbb{E}\{e^* \hat{h}\} = 0$ holds, i.e., e and $\hat{h}$ are orthogonal [92], [93]. To account for the non-orthogonal channel estimation errors for arbitrary linear channel estimators, we can construct an equivalent channel estimation error term z which is independent of $\hat{h}$. Here, we choose the channel estimation error model as in [94]

$$h = a\hat{h} + z \,, \tag{3.1}$$

where $a = \rho \frac{\sigma_h}{\sigma_{\hat{h}}}$ is the biasing factor and z is the equivalent estimation error term with zero mean and variance $\sigma_z^2 = (1 - |\rho|^2)\sigma_h^2$. We note that a popular LS channel estimation error model can also be included in (3.1) as a special case with a zero-mean channel estimation error due to the noise which is independent of h. For the LS channel estimation model, we find

that $\rho = \sigma_h / \sqrt{\sigma_h^2 + \sigma_e^2}$, where σ_e^2 is the variance of e. Thus, for the case of LS estimation, our model in (3.1) reduces to

$$h = \frac{\sigma_h^2}{\sigma_{\hat{h}} \sqrt{\sigma_h^2 + \sigma_e^2}} \hat{h} + z \ , \tag{3.2}$$

where the biasing factor becomes $a = \rho^2$, and z has zero mean and variance $\sigma_e^2 \sigma_h^2 / [\sigma_h^2 + \sigma_e^2]$. If the error e and channel c are correlated to each other, then the biasing factor becomes $a = \mathbb{E}\{\hat{h}^* h\} / \sigma_{\hat{h}}^2$ and the same channel estimation error model can still be valid.

3.2.1 Orthogonal Pilots

Most of the practical communications systems include certain known data structures in their transmission frames, called "training" or "pilot" signals. These are typically used for channel estimation and synchronization purposes. Accordingly, the pair of I/Q modulated channel coefficients g_k and g_{-k} in (2.7) at each subcarrier index k can be estimated either separately or jointly, using a known sequence of pilots.

Here, we consider a receiver where there is a simple BPSK pilot structure to mitigate the effect of the I/Q imbalance on the channel estimation. The transmission channel and the I/Q imbalance are supposed to be approximately time invariant for the duration of at least two OFDM symbols, we can write the pilot symbol matrix on a subcarrier for two consecutive OFDM symbols as

$$\mathbf{X}_p = \begin{bmatrix} x_{1,k} & x_{1,-k}^* \\ x_{2,k} & x_{2,-k}^* \end{bmatrix} \ , \tag{3.3}$$

These are selected so that $\mathbf{X}_p$ becomes non-singular for each mirror subcarrier pair, i.e., $\mathbf{X}_p \mathbf{X}_p^H = \alpha \mathbf{I}$ where α is the normalization factor. A simple BPSK selection maintaining the orthogonality between subcarriers is based on a Walsh-Hadamard matrix [79, 80, 60], $x_{j,k} = 1$, $x_{1,-k} = -1$ and $x_{2,-k} = 1$. This argument can be extended for the MIMO case as in [23, 5]. The orthogonality between the subcarrier k and $-k$ and between the different transmitter branches is achieved by distributing the same pilot structure in the space-frequency domain.

3.2.2 Effect of Channel Estimation

Joint estimation and equalization are assumed in the presence of transceiver I/Q imbalance. Both I/Q modulated channel pairs g_k / g_{-k} (2.7) on sub-

carrier and $\bar{g}_k = g_k(h_k \rightarrow h_{-k})/\bar{g}_{-k} = g_{-k}(h_k \rightarrow h_{-k})$ on its mirror need to be estimated, and the equalization process can be modeled as

$$\hat{\mathbf{x}} = \mathbf{x} + \hat{\mathbf{H}}^{-1}\mathbf{Z}\mathbf{x} + \hat{\mathbf{H}}^{-1}\mathbf{n} \ . \tag{3.4}$$

Pilots are selected such that $\det(\hat{\mathbf{H}}) \neq 0$, for $\hat{\mathbf{H}}$ to be non-singular. The estimated data vector $\hat{\mathbf{x}}$ and transmitted symbol vector $\mathbf{x}$ contain symbols on subcarrier and its mirror. Here, $\mathbf{n}$ is the I/Q corrupted noise vector and the estimated channel matrix $\hat{\mathbf{H}}$, estimation error matrix $\mathbf{Z}$ are

$$\hat{\mathbf{H}} = \begin{bmatrix} a_k\hat{g}_k & a_{-k}\hat{g}_{-k} \\ a_k\hat{g}^*_{-k} & a_k\hat{g}^*_k \end{bmatrix}, \ \mathbf{Z} = \begin{bmatrix} z_k & z_{-k} \\ \bar{z}^*_{-k} & \bar{z}^*_k \end{bmatrix} \ . \tag{3.5}$$

From (3.1), the biasing factors of the wanted and interfering channel components g_k and g_{-k} are denoted by a_k and a_{-k}. Consequently, they can be evaluated as a function of I/Q imbalance parameters and would be $a_k = \left[1 + \frac{(1+L)}{2(|K_{1,T}|^2+L|K_{2,T}|^2)\gamma_p}\right]^{-1}$ and $a_{-k} = \left[1 + \frac{(1+L)}{2(L|K_{1,T}|^2+|K_{2,T}|^2)\gamma_p}\right]^{-1}$ where γ_p is the SNR of the pilot transmission and L is the ILR at the receiver. Figure 3.1 shows the behavior of the biasing factors a_k and a_{-k} for the joint channel estimation. Note that the level of I/Q imbalance on both the transmitter and receiver sides are characterized by the ILR $L = [-25, -55]$dB. By considering the magnitudes of the I/Q imbalance coefficients on the given L values, one can approximate $a_k \approx \left[1 + \frac{1}{2\gamma_p}\right]^{-1}$. Hence, the effect of L is insignificant and the AWGN term dominates the performance and the biasing factor for the wanted part of the channel converges to unity at a high SNR. The biasing factor on the interfering channel can be written as $a_{-k} \approx \left[1 + \frac{1}{2L|K_{1,T}|^2\gamma_p}\right]^{-1}$. With a finite L, a_{-k} converges to unity for a sufficiently large SNR - that is when I/Q starts to dominate over thermal noise. For an ideal receiver with $L = 0$, I/Q never dominates over thermal noise, and $a_{-k} = 0$ always. Furthermore, the variance of the independent noise error converges to zero while the biasing factor tends to unity. Hence, at a high SNR where the estimator does indeed equal the actual channel response, the error starts to disappear. Afterwards, the performance of both the actual and the estimate lie on top of each other, although they exhibit a performance gap with a low SNR Publication I.

Figure 3.2 demonstrates how the SER performance degrades with the imperfect channel estimation of the ZF equalization. The effect of channel estimation is simulated with Gaussian approximated mirror carrier interference as well [38]. From Figure 3.1, it is clear that the biasing factor a does not have any significant impact on system performance. For the

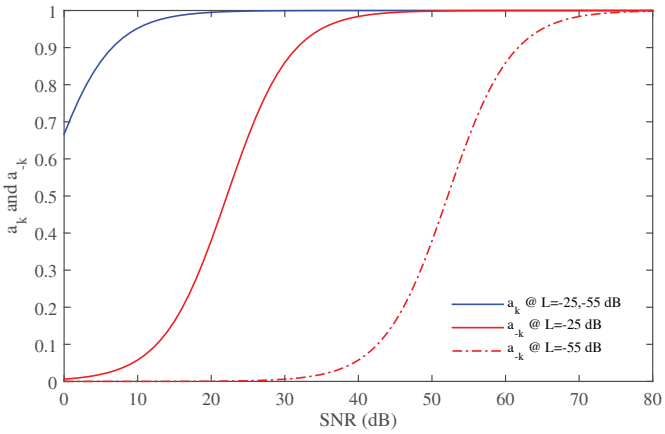

Figure 3.1. Behavior of the biasing factors a_k and a_{-k} for the joint channel estimation for the ILRs of $[-25,\ -55]$dB. Pilots are selected from BPSK alphabet. I/Q mismatches are chosen as $g = [0.9,\ 1]$ and $\phi = [2,\ 0.2]^\circ$, respectively for above ILR values.

relatively small L, $a \rightarrow a_{ideal} = [1 + \frac{\sigma_p^2}{\sigma_h^2}]^{-1}$, where a_{ideal} is the biasing factor of an ideal receiver, this again emphasizes the above facts. At a higher SNR, the estimation error term z ($\sigma_z^2 = (1-a)\sigma_h^2$) converges to zero while the biasing factor tends to unity. Therefore, the imperfect channel estimation follows the equalization with perfect channel knowledge at higher SNR values. The performance of the Gaussian approximated system exhibits slightly worse error floors with higher order modulations. However, it is reasonable to assume that the mirror carrier interference is Gaussian distributed, especially for low-order modulation schemes.

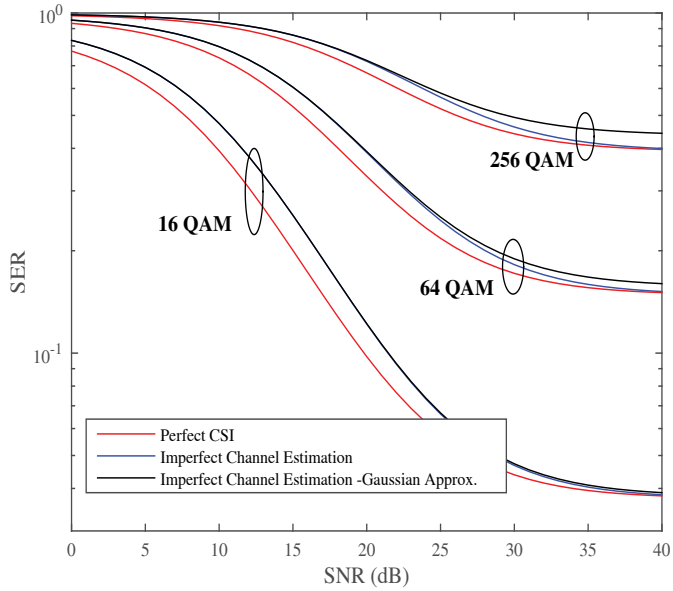

Figure 3.2. The SER for M-QAM modulations ($M = 16, 64, 256$) of ZF equalization with perfect channel knowledge, imperfect channel estimation and with Gaussian approximated mirror carrier interference at $L = -25$dB ($g = 0.9$ and $\phi = 2°$) for both transmitter and receiver.

4. MIMO-OFDM Coding with I/Q Interference

Wireless environments present a challenging communications problem because of possible time-, frequency- and spatially-varying degradation caused by signal fading. These impairments are not necessarily harmful. Under certain conditions, it is possible to take advantage of such variations in the channel's responses to improve the received SNR. The method for achieving reliable transmission over such fading channels is called *diversity*.

Open loop diversity methods enable the receiver to recover a more robust replica of the transmitted signal by combining a number of independently faded copies in a situation where there is no CSI at the transmitter. Diversity can generally be obtained by transmitting information, either in different time slots, at different frequencies, with different polarizations or from different antennas.

Using different time slots which are separated for more than the coherence time of the channel leads to so-called "temporal diversity" [95]. Copies of the transmitted signal are sent over these time slots and suitable error-correcting codes can be utilized to reduce the amount of redundancy. However, in slow fading, the coherence time of the channel is large and temporal diversity methods are not practical.

Signal copies transmitted from different carrier frequencies achieve frequency diversity if the carrier frequencies are separated by more than the coherence bandwidth of the channel.

Spatial diversity uses multiple antennas separated by at least half of the wavelength to achieve diversity, and thus multiantenna techniques have become a trend in modern wireless communications systems.

Concurrently with space-time coding, the principles of spatial multiplexing were also formulated [96]. The basic principle behind spatial multiplexing is to transmit different symbols from each antenna, and have the

receiver detect these symbols by taking advantage of the fact that each transmit antenna has a different spatial signature at the receiver. This does allow for an increased number of information symbols per MIMO symbol, but it does not enhance reliability.

In closed loop methods, CSI is available at the transmitter. In Closed loop MIMO-systems, linear precoding in which the signal is transmitted on the dominant modes of the channel matrix, can be used to further improve system performance by tailoring the transmission to the instantaneous channel conditions [97, 98] while retaining the benefits of all-linear processing. Since OFDM uses multiple subcarriers, optimal precoding for MIMO-OFDM can be achieved by deriving precoders for each subcarrier independently or for a group of adjacent subcarriers with almost identical channels.

In Time Division Duplex (TDD) systems, CSI may be faithfully estimated at the transmitter using channel reciprocity. When the reciprocity of wireless channels does not hold, such as in Frequency Division Duplex (FDD) systems, a feedback link is needed for providing CSI to the transmitter [99, 100].

Transmit beamforming with receiver combining is one of the simplest approaches to achieve full diversity [101]. Compared with traditional space-time/frequency codes, beamforming and combining systems provide diversity as well as array gain at the expense of requiring CSI at the transmitter in the form of a transmit beamforming vector. To achieve high rates for users, multistream precoding methods are needed [98]. Moreover, for downlink MU systems, complete processing at the receiver may not be possible and transmitter precoding techniques necessarily play a major role.

Recently, the combination of multiantenna techniques and OFDM has drawn attention in communications and signal processing. The non-idealities due to I/Q imbalance can cause a considerable decrease in the overall system performance. In this chapter, mutliantenna coding methods used in OFDM systems suffering from I/Q imbalance are discussed. Detailed discussions can be found in Publication II,Publication III

4.1 Diversity in an I/Q-distorted environment

4.1.1 Space-Time Coding in the I/Q Domain

Multiple antenna transmission and reception has emerged as a key tool in achieving high levels of spectral and power efficiency in wireless communications. Signaling schemes that exploit both the classical Shannon degrees of freedom (time-frequency) and the additional spatial degrees of freedom (antennas) without using CSI at the transmitter are referred to as Space-Time Codes (STC) [102]. OFDM modulation with a cyclic prefix can be used to transform frequency selective fading channels into multiple flat fading channels so that orthogonal space-time transmitter diversity can be applied, even for channels with large delay spreads. For a fixed number of transmit antennas, decoding complexity increases exponentially with the transmission rate. Alamouti [103] discovered a remarkable scheme for transmission over two antennas which is much less complex than the space-time trellis code [102]. The Alamouti scheme provides full diversity and rate-one transmission for complex constellation symbols with maximum-ratio receiver combining. The Alamouti code is an orthogonal Space-Time Block Code (STBC) for two transmit antennas. Subsequently, it is widely used in wireless communications standards, such as WCDMA.

The I/Q distortion increases the probability of error in a given transmission significantly and should be efficiently mitigated. A digital signal processing technique to mitigate the I/Q distortion in an Alamouti coded STBC-MIMO-OFDM transmission has been investigated in [11] . In addition to the Alamouti code STBC, quasi-orthogonal and rotated constellation quasi orthogonal cases were considered for different antenna configurations in [22]. An analytical framework for evaluating receiver SINR performance was studied for MISO-OFDM in [104] and the capacity and rate performance were discussed in [35] for the joint effect of other impairments. Pilot based and blind digital compensation techniques for STC multiantenna systems with flat I/Q imbalance were considered in [23], while for frequency selective I/Q imbalance, compensation techniques were studied in [105].

4.1.2 Space-Frequency Coding in I/Q Domain

As an alternative to space-time coding, Space Frequency Block Coding (SFBC) is an attractive solution for OFDM systems. In SFBC, the symbols are distributed across the space (antennas) and frequency (OFDM tones) [106, 107]. In these, existing STBCs were used, replacing the time domain symbols with frequency domain subcarriers. Compared to STBC-OFDM, SFBC-OFDM has the advantage that transmissions do not spread across multiple symbols, and accordingly they are more robust to Doppler effects. Such SFBC-OFDM is an effective technique for achieving full transmitter diversity, especially for applications where the normalized Doppler frequency is large. An SFBC based on the Alamouti code is used in LTE [108].

Meanwhile, it has been proven that the Alamouti scheme across tones fails to exploit frequency diversity when considering fading effect and these codes will generally be sub-optimum when employed as space-frequency codes [109, 110]. The authors in [109, 111] reported that a MIMO-OFDM with space-frequency system can achieve a maximum diversity gain in the frequency selective channel as long as the channel correlation matrix is full rank.

The performance of an SFBC-OFDM system suffers from I/Q imbalance. A digital pilot based I/Q mitigation scheme is considered for an Alamouti coded SFBC-OFDM [44]. A properly designed SFBC may compensate for the I/Q imbalance. In [24], a group linear constellation pre-coded scheme is suggested. A precoder for mapping symbols on the mirror subcarrier pairs is used together with an Alamouti SFBC. The resulting code is 4×4 SFBC. An Alamouti SFBC transmission on two neighboring subcarriers is coupled by the precoding with an Alamouti transmission on the mirror carriers.

Furthermore, Alamouti coding over the mirror subcarriers efficiently cancels ICI caused by the I/Q imbalance without any additional signal processing Publication II. Three different subcarrier allocations are suggested there and are summarized below in Table 4.1.

A generalized SFBC-MIMO-OFDM signal model with receiver I/Q distortion can be represented as

$$\mathbf{y} = \mathbf{H}_e \mathbf{s} + \mathbf{n}_e \ , \tag{4.1}$$

where $\mathbf{H}_e$, $\mathbf{y}$, $\mathbf{s}$ and $\mathbf{n}_e$ are the effective channel matrix, the received signal vector, the transmitted symbol vector and the effective noise vector, re-

Table 4.1. SFBC schemes proposed in Publication II.

Coding across mirror subcarriers.				
Transmit Antenna	k	$k+1$	$-k-1$	$-k$
1	s_1	s_3	$-s_4^*$	$-s_2^*$
2	s_2	s_4	s_3^*	s_1^*
Coding across adjacent subcarriers.				
Transmit Antenna	k	$k+1$	$-k-1$	$-k$
1	s_1	$-s_2^*$	s_3	$-s_4^*$
2	s_2	s_1^*	s_4	s_3^*
Coding across adjacent subcarriers with a single subcarrier shift.				
Transmit Antenna	k	$k+1$	$-k-2$	$-k-1$
1	s_1	$-s_2^*$	s_3	$-s_4^*$
2	s_2	s_1^*	s_4	s_3^*

spectively. Note that the received signal vector $\mathbf{y}$ contains the stack of receiving signals on both subcarrier and its mirror. These matrices depend on the type of transmission. The effective channel and noise matrices can be further decoupled as $\mathbf{H}_e = \mathbf{KH}$ and $\mathbf{n}_e = \mathbf{Kn}$, respectively, where $\mathbf{K}$ is the matrix describing the receiver I/Q imbalance effect. The matrices $\mathbf{H}$ and $\mathbf{n}$, respectively, represent the actual channel matrix and the noise vector.

Table 4.1 shows three SFBC schemes proposed in Publication II. The two pairs of complex-valued symbols (s_1, s_2) and (s_3, s_4) are mapped across: i) mirror subcarriers ii) adjacent subcarriers, and iii) adjacent subcarriers with a single subcarrier shift. It can be seen that a distinguishing feature of the proposed new scheme i) is that it cancels the receiver I/Q imbalance automatically without additional signal processing if the pilot symbols are coded also in the same manner. The SFBC scheme ii) [112, 44] introduces I/Q interference among four symbols, such that each the four symbols coupled by the I/Q imbalance is detected jointly. The previous SFBC scheme is slightly modified and distributed over the adjacent subcarriers into the upper and lower halves of the OFDM symbol with a single subcarrier shift (for further details, refer to Publication II-Table IV). In the considered case, the I/Q interference disturbing a coding block comes from two adjacent coding blocks in the mirror half. With this arrangement, the interference experienced due to the I/Q imbalance has the same average

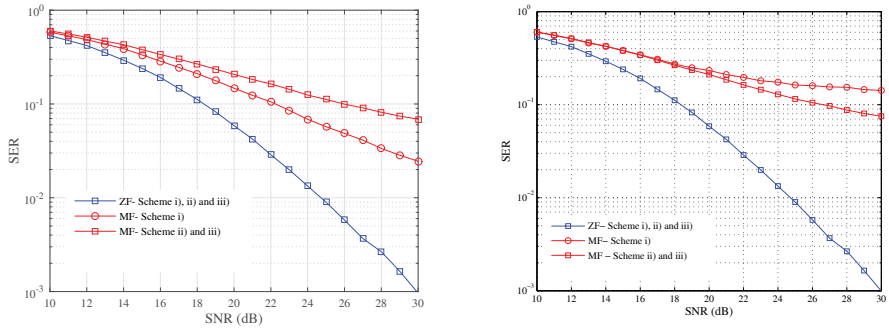

Figure 4.1. SER performance for the proposed SFBC schemes. Left: Flat fading. Right: Pedestrian A channel with coherence bandwidth $= 4.4$MHz. ILR, $L = -25$dB ($g = 0.9$ and $\phi = 2°$) and 64-QAM modulation is considered with 2×1 OFDM system with 256 active subcarriers (15kHz subcarrier spacing).

power as the previous scheme but the interference term contains more components. The joint detection of the coupled subcarriers in this scheme is much more difficult due to the convoluted nature of the interference.

To understand the real effect of I/Q imbalance under the various receiver configurations, the self-interference, other symbol interference and noise covariance matrices need to be known. For performance comparison of the above SFBC with different receiver configurations, the channel and the noise covariance matrices are considered for the frequency flat channel. The effective channel covariance matrix for a given channel realization of the signal model described in (4.1) for the SFBC scheme i), can be computed as $\mathbf{R}_h = \mathbf{H}_e^H \mathbf{H}_e = a\mathbf{I} + \mathbf{B}$, where

$$\mathbf{B} = \begin{bmatrix} \alpha & \beta \\ \beta^* & -\alpha \end{bmatrix} \tag{4.2}$$

with $a = |h_1|^2 + |h_2|^2$, $\alpha = 2\Re\{h_1 h_2 \epsilon^*\}$ and $\beta = h_2^2 \epsilon^* - h_1^{*2} \epsilon$. Here, h_i is the channel on the ith transmission and $\epsilon = \frac{2K_{2,R}K_{1,R}^*}{|K_{1,R}|^2+|K_{2,R}|^2}$. It is clear that the receiver I/Q imbalance introduces non-orthogonality between channels and leads to self interference among the symbols.

When the equivalent channel is invertible, as in our case, the noise covariance matrix for the ZF receiver, $\mathbf{R}_n = \mathrm{N}_0(\mathbf{H}^{\mathrm{H}}\mathbf{H})^{-1}$, can then be reduced to $\mathbf{R}_n = \mathrm{a}\mathbf{I}$, and the ZF receiver removes the cross interference between channels - which emphasizes the flat fading characteristics - and it removes the I/Q effect on the channel noise as well. Similarly, for the scheme ii) with an MF receiver, the channel covariance matrix would be

$$\mathbf{R}_h = \begin{bmatrix} a\mathbf{I} & \mathbf{B} \\ \mathbf{B}^H & a\mathbf{I} \end{bmatrix}. \tag{4.3}$$

We can observe a significant effect: the contribution of I/Q imbalance is limited to the off-diagonal, and the I/Q interference is limited to the mirror carriers. The noise covariance matrix for the ZF receiver is almost similar to (4.3) and the off-diagonal elements are scaled by a factor of two. Figure 4.1 shows the SER performance of the above SFBC schemes over frequency flat and Pedestrian A channels. As the ZF reception removes the effect of receiver I/Q imbalance completely, the performance exhibits significant improvement independent of the SFBC structure. For the schemes ii) and iii) with the MF receiver, the performance become worse and thus the interference leaking from the mirror subcarrier pair instead dominates the self interference from its own subcarrier pair in the first scheme. Note that the MF discussed here is based on a white noise approximation of joint interference, i.e. the algorithm does not take into account potential variations of the interference powers in different diversity branches, and combines coherently the samples of the symbols of interest. In the mildly selective Pedestrian A channel, the ZF receiver is able to compensate for non-orthogonality, but performance of the MF receiver is poor. Furthermore, either Alamouti code distributes over two antennas, receiver observes only two independent faded versions of a given symbol irrespective of the fading scenario. Hence, the expected diversity order would be two, and MF receiver here, looses diversity benefits due to non-orthogonality induced by I/Q imbalance when the channel becomes frequency selective. Publication Publication II provides a comprehensive study of the performance characteristics in different fading situations.

4.2 Precoding in I/Q Domain

MIMO-OFDMA plays a remarkable role in modern wireless systems such as LTE [108]. In order to take full advantage of this scheme, limited availability of frequency spectrum, availability of total transmit power and the nature of wireless channels have to be well addressed. A dynamic resource assignment scheme allocates a dimension adaptively to different users according to their current and effective channel gains while a fixed resource allocation assigns them irrespective of the current channel condition. In future communication systems greater attention has been paid to the trade-off between system capacity and fairness among the users [113, 114].

In MIMO-OFDMA, sets of subcarriers are allocated for users according

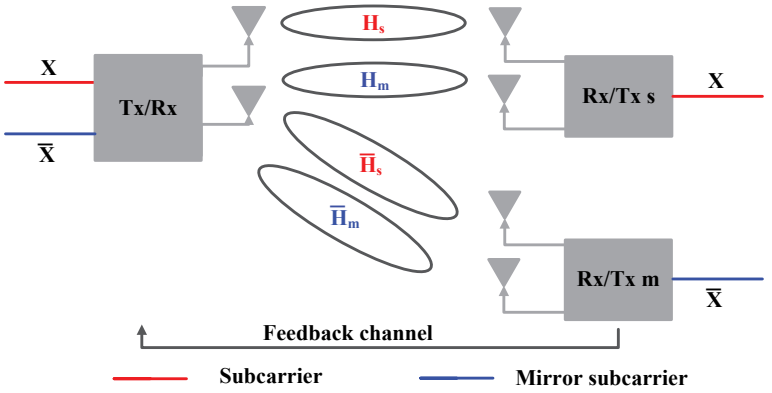

Figure 4.2. An MIMO-OFDMA system model on a mirror subcarrier pair.

to the demand and the instantaneous channel state. Hence, transmissions to users scheduled on mirror subcarriers interfere with each other due to I/Q imbalance, and precoders selected on a carrier affect the I/Q interference experienced at the mirror carriers. Therefore, at a high SNR, it becomes essential to study the joint selection of precoders for a subcarrier and its mirror.

Similar interference situations emerge in coordinated multipoint transmission scenarios [115, 116]. Related to I/Q imbalance, two-cell interference alignment [116] or coordinated beamforming is of particular interest. In [27], the authors came across with an expression for the outage probability of beamforming OFDM systems with transmit and receive I/Q imbalances. Moreover, the asymptotic behavior and diversity order of the system is investigated. Instead of coordinated transmission in interfering two cells, the authors in Publication III,[10] consider coordinating transmission on two interfering carriers.

Let us consider a downlink of a $M_T \times M_R$ MIMO OFDMA system and potentially multiple users. Both transmitters and receivers experience the effect of frequency flat I/Q imbalance. Each user is assigned subcarriers depending on its demand and the precoders acting on them are selected based on channel information conveyed to the transmitter over an infinite rate feedback channel. We assume that transmissions on a subcarrier s and its mirror m are widely separated in frequency, and hence, fading across these subcarriers is independent. The I/Q-corrupted received symbol on subcarrier s is then described by

$$\mathbf{y}_s = \mathbf{H}_s\mathbf{W}\mathbf{x} + (\epsilon_T^*\mathbf{H}_s^* + \epsilon_R\mathbf{H}_m)\overline{\mathbf{W}}^*\overline{\mathbf{x}}^* + \mathbf{n}_s + \epsilon_R\mathbf{n}_m^* \ , \tag{4.4}$$

where $\mathbf{H}_s$ and $\mathbf{H}_m$ are the channel matrices on the subcarrier and its mir-

ror between the transmitter and the receiver scheduled on the subcarrier s. Similarly, $\bar{\mathbf{H}}_s$ and $\bar{\mathbf{H}}_m$ are the channel matrices on mirror m as illustrated in Figure 4.2. The precoding matrices on the subcarrier and its mirror are denoted by $\mathbf{W}$ and $\overline{\mathbf{W}}$, respectively. The transmitted symbols for the users scheduled on the subcarrier and its mirror are represented by $\mathbf{x}$ and $\bar{\mathbf{x}}$. The AWGN noise samples on the mirror carriers are $\mathbf{n}_s$ and $\mathbf{n}_m$. The transmitter and receiver I/Q imbalances are characterized by the complex coefficients ϵ_T and ϵ_R. Note that, as the user scheduled on subcarrier s differs from the uses scheduled on m, the precoder $\overline{\mathbf{W}}$ is selected according to $\bar{\mathbf{H}}_m$ and not according to $\mathbf{H}_m$.

We assume unitary precoding. With white noise, the optimal receiver is a matched filter based on eigenbeam combining. If the mirror carrier transmission is not full rank, an eigenbeam combiner would no longer be optimum, as the interference would be colored. Here, we however assume I/Q-blind reception and combine the received signals using a simple MF receiver. Now, the post processing SINR for MIMO stream k of the subcarrier transmission can be written as

$$\gamma_k = \frac{(\mathbf{w}_k^H \mathbf{R}_s \mathbf{w}_k)^2}{||\mathbf{w}_k^H \tilde{\mathbf{H}}_s \overline{\mathbf{W}}^*||^2 + (1+|\epsilon_R|^2) N_0 \mathbf{w}_k^H \mathbf{R}_s \mathbf{w}_k} \quad , \tag{4.5}$$

where $\mathbf{R}_s$ and $\mathbf{R}_m$ are the covariance matrices of $\mathbf{H}_s$ and $\mathbf{H}_m$, respectively. Here, the channel carrying I/Q interference is $\tilde{\mathbf{H}}_s = (\epsilon_T \mathbf{H}_s^H \mathbf{H}_s + \epsilon_R^* \mathbf{H}_s^H \mathbf{H}_m^*)$. A similar approach can be applied to derive the SINR of the mirror subcarrier transmission. For simplicity, let us focus on a 2×2 system with single stream transmissions on both subcarriers.

The selection of the precoders can be done in different ways and four alternatives are considered Publication III.

- Prioritizing Subcarrier Transmission: The SINR of the subcarrier transmission can be maximized by maximizing the own signal power and minimizing the I/Q interference induced due to the mirror carrier transmission. Maximum signal power can be achieved by selecting a precoder on the subcarrier $\mathbf{w}$ which exactly matches the strongest eigenvector of the channel covariance matrix $\mathbf{R}_s$; thus, $\mathbf{w} = \mathbf{w}^P = \mathbf{V}^{(1)}$. Accordingly, the mirror carrier precoder $\overline{\mathbf{w}}$ would be

$$\mathbf{w}^I = \arg \min_{\overline{\mathbf{w}}, ||\overline{\mathbf{w}}||=1} \left(\mathbf{w}^H \mathbf{H}_s^H \tilde{\mathbf{H}}_s^* \overline{\mathbf{w}}^* \right) \quad , \tag{4.6}$$

  which induces zero interference with the desired transmission. A similar argument can be applied for the mirror carriers transmission.

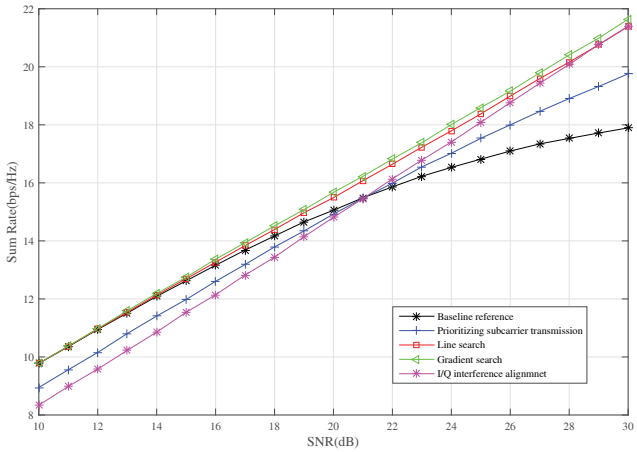

Figure 4.3. Sum-rate performance comparison for different precoder selection schemes. Single stream precoded 2×2 MIMO transmission on two independently fading subcarriers to two users, subject to Tx and Rx I/Q imbalance with $L = -25$dB ($g = 0.9$ and $\phi = 2°$).

- Iterative Line Search: Instead of prioritizing one of the subcarriers in the mirror carrier pair, the precoders can be obtained using a line search along the two extremes $\mathbf{w}^P$ and $\mathbf{w}^I$ [117].

$$\mathbf{w} = \alpha \mathbf{w}^P + (1 - \alpha)\, \mathbf{w}^I, \quad ||\mathbf{w}|| = 1 \tag{4.7}$$

  The precoders on a mirror carrier pair can be selected by tuning α to achieve a maximum sum rate.

- Iterative Gradient Search: The sum rate is a monotonically increasing function of the SINRs, and it is sufficient to maximize $\prod(1 + \gamma_k)$ to obtain a set of precoders which maximize the sum rate. Note that the partial derivative can be written as a linear function of individual partial derivative terms with regard to the precoder $\mathbf{w}$ and its complex conjugates $\mathbf{w}^*$ [118].

- I/Q Interference Alignment: The I/Q interference can be perfectly removed by selecting the precoder $\overline{\mathbf{w}}$, which is a generalized eigenvector of $\mathbf{H}_s^H \tilde{\mathbf{H}}_s^*$ and $\tilde{\mathbf{H}}_m^H \mathbf{H}_m^*$ respectively. The channel $\tilde{\mathbf{H}}_m^H$ is the I/Q interference bearer.

Figure 4.3 shows the sum rate performance for the above precoder selection schemes for a 2×2 MIMO transmission on OFDMA subcarrier pairs under $L = -25$dB. Single-stream precoding is applied on both subcarriers.

The baseline scheme selects precoders separately, where the precoder is selected as the maximum eigenvalue eigenvector on both carriers. The precoder selection where $\mathbf{w}_s$ is selected to maximize the received power of the subcarrier transmission, and $\mathbf{w}_m$ is selected to minimize the power from the mirror subcarrier to the corresponding subcarrier, referred to as "prioritizing subcarrier transmission". The performance is better than the baseline reference when the I/Q interference dominates at high SNR region. In this scheme, I/Q interference is completely removed from one of the transmissions, whereas the other transmission suffers from random I/Q interference. Iterative line and gradient search precoders jointly maximize the sum rate, while a priori favoring neither of the transmissions. Line and gradient searches show similar performance at low SNR values. Gradient search slightly outperforms line search at a high SNR. This indicates that, in this single-stream precoding case, the sum-rate optimal precoders are not linear combinations of power maximizing and interference minimizing precoders, but rather are closely approximated by such. As expected, the joint interference alignment performs poorly at a low SNR when I/Q interference is irrelevant. At a high SNR, when I/Q interference is potentially stronger than the channel noise, it achieves the same performance as iterative line search.

5. Interaction of I/Q Interference and Radio Resource Management

Recently, there has been much interest in cross-layer designs, where one allows the physical layer to interact and share information with higher layers to achieve significant performance gains [119, 120, 121]. To improve performance measures such as system capacity, data rate, coverage reliability, and QoS, implementing a system level control of co-channel interference and other radio transmission characteristics in wireless communications systems through Radio Resource Management (RRM) is essential. RRM involves strategies and algorithms for controlling parameters such as transmit power, scheduling, beamforming, data rates, handover criteria, modulation and error coding schemes, and managing interference between different transmissions and cells. The objective is to utilize the limited radio frequency resources and radio network infrastructure as efficiently as possible.

Dynamic RRM schemes adaptively adjust the radio network parameters according to the traffic load, user positions, user mobility and QoS requirements. Dynamic RRM schemes play a major role in designing wireless communications systems, in view to minimize expensive manual cell planning and achieve optimize frequency reuse, resulting in improved system spectral efficiency.

Link adaptation and power control are widely used RRM tools to guarantee reliable operation of a communication system. Initially, link-adaptation in an ideal system with an infinite granularity of modulation and coding schemes is discussed when there is an uncompensated I/Q interference exists. Latter part of the section demonstrates the I/Q induced near-far effect in a situation where cellular and D2D transmissions happen on orthogonal mirror frequency resources while prioritizing cellular transmission by applying FPC to the D2D users, effectively mitigating excessive interference radiating from D2D communication.

5.1 I/Q Aware Link Adaptation

The basic idea of link adaptation is to adapt the transmission characteristics on a link to the actual channel conditions by varying certain transmission parameters, essentially transmission power, the data rate, the constellation size and the coding scheme. With the selection of these transmission parameters, the system makes the most out of a time varying channel, instead of fixing the parameters for a worst-case channel. The trade-off involves minimizing the error probability for robustness and maximizing the instantaneous throughput for bandwidth efficiency. When I/Q interference is present in the system, its characteristics may be taken into account in link adaptation, to enhance its accuracy.

5.1.1 Adaptive Modulation and Coding

In AMC, the transmission rate on a link is adapted according to the link quality, to counteract fading and enhance the performance of wireless systems [122, 123]. Within the AMC scheme, a Channel Quality Indicator (CQI) is usually employed to feedback an index of an appropriate Modulation and Coding Set (MCS) with which the maximum throughput is expected. The estimation of which MCS can be supported is based on the expected SINR at the time of transmission. In CQI generation, channel variations can greatly impact the performance of adaptive codes, even in systems with low mobility and small delay between the channel estimation and data transmission [124]. In order to cope with this degradation, CQI generation based on mean mutual information has been proposed for OFDM systems with AMC [125, 126]. The autocorrelation of the fading process dictates the rate of channel variation and how often the transmitter must adapt its transmission.

The implementation of AMC offers several challenges. In constantly varying mobile channels, delays in reporting reduce the reliability of the CQI measurements, creating outdated CSI. Further, errors in the channel estimate can lead the scheduler to select the wrong transmission parameters, wasting system capacity or raising the Block Error Rate (BLER). To provide protection against such transmission failures, wireless communications systems require re-transmission protocols and error-control/correction schemes at the physical layer. Combining AMC with an Automatic Repeat Request (ARQ) or Hybrid ARQ (HARQ) enhances the system throughput by allowing the retransmission of erroneous packets and packet com-

bining while reducing the number of required MCS levels and the sensitivity to measurement error and traffic fluctuations [127].

The presence of unexpected interference leads to measurement errors and is a possible cause of performance degradation. An OFDM system, with fast adaptive modulation which tracks small-scale fading in the presence of interference, was investigated in [128], and a slow, adaptive modulation technique was proposed in a co-channel interference situation [129]. A discrete rate link adaptation scheme is proposed to maximize the average spectral efficiency of the cognitive radio, while minimum average spectral efficiency for the primary user is provisioned [130]. The AMC mode selection and TPC at the cognitive transmitter are optimized based on the SINR of both links. A similar variable-rate, variable-power scheme employed under delay Quality of Service (QoS) constraints can be found in [131].

Uncontrolled variability in interference is caused by beamforming transmissions in multicellular systems. In [132], it was argued that the effects of such interference variability were insignificant, being induced by the non-idealities of the system. However, the a priori weak interference caused by I/Q interference may have more damaging effects on MIMO-OFDMA system performance.

In the context of precoded MIMO in a multicellular system, the so-called "flashlight effect" has been discussed [132, 133], varying due to changes in precoding at an interferer. To properly select a transmission mode in a situation with SINR variability, it is essential to know its statistics. Optimal link adaptation with respect to channel quality misprediction due to time selective fading has been addressed in [134], and jointly so for time selective fading, channel estimation errors and the flashlight effect in [133]. In [134, 133, 132], link adaptation with a finite set of modulation and coding schemes was considered. If one assumes a link adaptation scheme with an infinite granularity of ideal modulation and coding schemes [123, 135, 134], that amounts to knowing the pertinent capacity of the link subject to fading according to the SINR statistics. In an AMC/HARQ system with CQI errors, rate adaptation was analyzed by assuming the awareness of the underlying channel distribution and BLER [136].

5.1.2 AMC in I/Q-Distorted Precoded MIMO-OFDMA

When precoding is used in MIMO-OFDM, I/Q imbalance limits the precoding gains [27],[10]. Optimally, to compensate for the I/Q imbalance, the precoders on a carrier and its mirror should be jointly selected Publication III,[123]. If precoding is not jointly optimized in precoded MIMO-OFDM(A), changes in the precoding on a carrier cause non-controlled variation in the SINR experienced by the interference victim on the mirror carrier due to the I/Q imbalance. This may cause mispredictions of the channel quality, wrong link adaptation decisions and accordingly losses of transmissions.

Here, we study AMC in a precoded MIMO-OFDMA system, depicted in Figure 4.2. For simplicity, we concentrate on analysing downlink OFDMA transmissions, with results readily generalizable to uplink, and OFDM. The channels are corrupted by I/Q interference both at the transmitter and the receiver.

In OFDMA, it is sufficient to concentrate on analysing a subcarrier s of interest, and its mirror subcarrier m. On the subcarrier of interest, the rank-p precoder $\mathbf{W} \in \mathbb{C}^{M_T \times p}$ is used, and on the mirror the rank-q precoder $\overline{\mathbf{W}} \in \mathbb{C}^{M_T \times q}$ is used. The precoders are normalized as $\mathrm{Tr}\{\mathbf{W}^H\mathbf{W}\} = p$, and $\mathrm{Tr}\{\overline{\mathbf{W}}^H\overline{\mathbf{W}}\} = q$. The transmit symbol vector on subcarrier s is $\mathbf{x} \in \mathbb{C}^{p\times 1}$ and the symbol vector on its mirror m is $\bar{\mathbf{x}} \in \mathbb{C}^{q\times 1}$. Symbols are drawn from a complex Gaussian symbol constellation with power constraint, $\mathbb{E}_x\{\mathbf{x}\mathbf{x}^H\} = \frac{1}{\kappa}\mathbf{I}_\kappa, \kappa = p, q$. In downlink, the I/Q corrupted $N_R \times 1$ received signal vector on the subcarrier s of interest is given by (4.4). Using an eigenbeam combiner at the receiver, the post processing SINR of the kth eigenbeam is

$$\gamma_k = \frac{p_k \lambda_k}{\left\| \left(\epsilon_T^* \sqrt{\lambda_k} \left(\mathbf{v}_k\right)^H + \epsilon_R \left(\mathbf{u}_k\right)^H \mathbf{H}_m^* \right) \overline{\mathbf{W}}^* \right\|^2 + \frac{\left(1+\epsilon_R^2\right)}{\gamma_0}}. \tag{5.1}$$

Here, λ_k is the kth eigenvalue of the channel $\mathbf{H}_s$, and $\mathbf{u}_k$ and $\mathbf{v}_k$ denote the kth eigenvector of the left and right unitary matrices, respectively. The power allocation on eigenbeam k is given by p_k which represents the kth element of the diagonal power allocation matrix. The average SNR is γ_0 and the effect of the transceiver I/Q imbalance is characterized by $\epsilon_{T/R}$

In (5.1), the impact of the mirror precoder $\overline{\mathbf{W}}$is clearly visible. If the mirror transmission applies a full-rank unitary precoder, the SINR does not depend on the mirror precoder $\overline{\mathbf{W}}$. Otherwise, both the a priori unknown I/Q channels and the precoding affect the interference. This phenomenon

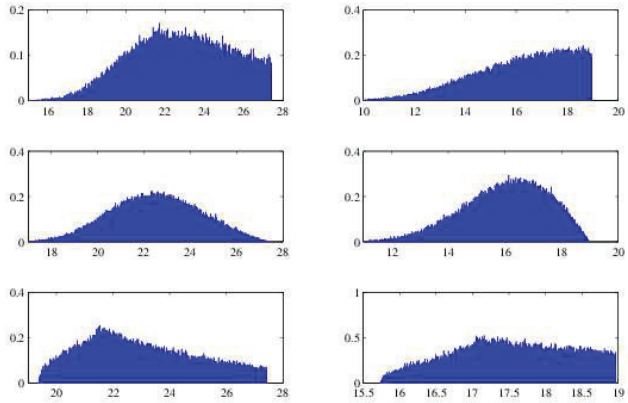

Figure 5.1. Simulated probability density of SINR [dB] in a 2×2 MIMO-OFDMA system. First row: rank one interference. Second row: rank two interference . In both, wanted channel $\mathbf{H}_s$ is randomly distributed. Third row: one instance with fixed $\mathbf{H}_s$, rank one interference. Left: a stronger eigenbeam. Right: a weaker eigenbeam.

can be defined as an *I/Q flashlight effect*.

Although eigenbeamforming is performed with perfect CSI at the transmitter, the I/Q interference varies depending on the mirror interference channel $\mathbf{H}_m$, as well as the user scheduled on the mirror subcarrier and its precoder $\overline{\mathbf{W}}$. This causes large fluctuations in the SINR observed at the receiver, as shown in Figure 5.1 for SNR=IRR=25dB and unitary precoding. For an example fixed channel realization (the third row of Figure 5.1), we observe a variation of 8dB in the SINR, depending on the mirror precoder and the mirror subcarrier channel. Accordingly, a rank- deficient precoded transmission on the mirror carrier causes an *I/Q flashlight effect* on the subcarrier of interest, analogous to the co-channel flashlight effect caused by precoding in other cells.

In Publication Publication IV, a link adaptation scheme with an infinite granularity of ideal modulation and coding schemes [123, 135, 134] in a system suffering from the I/Q flashlight effect has been investigated. Three transmission modes are considered:

- Joint Transmission (Tx) and Reception (Rx)
- Joint Tx and Separate Rx
- Separate Tx-Rx are selected.

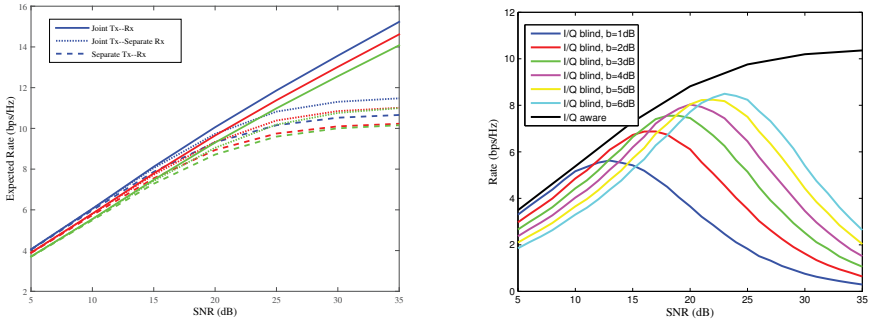

Figure 5.2. Throughput performance in a block fading downlink. Left: Expected throughput for the I/Q aware link adaptation for outage probabilities 1% (blue), 5% (red) and 10% (green). Right: Throughput for I/Q blind link adaptation for Separate Tx-Rx mode.

Ergodic and block fading channels are treated. Based on knowledge of the statistics of the I/Q interference, methods to choose MCSs providing reduced outage probabilities, and optimum expected rates are devised.

Figure 5.2 shows the expected rate performance as a function of the average SNR in 2×2 i.i.d. Rayleigh block fading channels. The three different transmission modes for I/Q aware link adaptation are considered at an outage probability [1, 5, 10]% with IRR = 25dB at Tx and Rx. Rates achieved by I/Q blind link adaptation through backoff values for Separate Tx-Rx mode is illustrated on the right side of the Figure. The I/Q interference is rank-one precoded and the interference is, accordingly, spatially colored. Hence, the receiver observes one dimension which does not see any I/Q interference at all. When the receiver performs joint decoding, the information transmitted on this dimension is corrupted only by noise, whereas the information transmitted on the orthogonal dimension is corrupted by the I/Q interference. At a high SNR, there is thus one high-SNR dimension remaining at the receiver. If information is jointly transmitted over the eigenbeams and jointly decoded, the capacity thus grows indefinitely. At a high SNR, the capacity does not, however, grow as a two-stream MIMO capacity but rather as a single-stream capacity. Separate reception results in relatively poor performance at a high SNR. Further discussion of this is available in Publication IV. Referring to this being the basic MIMO transmission method in LTE, one may learn that significant gains can be achieved with I/Q aware link adaptation.

5.2 I/Q Near-far Effect in Device-to-Device Communication

5.2.1 Device-to-Device Communication

Device-to-Device (D2D) communications underlying cellular networks is a promising solution to improve the throughput of cellular networks. The main idea in D2D-enabled cellular networks is to permit transceiver pairs to be close to each other to establish direct peer-to-peer connections between one another. The coexistence of D2D and cellular communications in the same spectrum poses a set of new technical challenges, including interference management, resource allocation, mode selection and TPC. For example, in an OFDM system in which D2D communications links may reuse some of the OFDM time-frequency resources, intra-cell interference is no longer negligible [137]. These new types of interference situations are intertwined with the duplexing scheme that the cellular network and the D2D link employ, and also depend on the resources allocated to D2D links.

Solution approaches to deal with this problem in particular include TPC- [138] and various interference management techniques [139] that can be combined with proper mode selection [140]. Both D2D and cellular communications can operate in multiple modes: non-orthogonal resource sharing where D2D communications can reuse the same resources used by cellular communications, and orthogonal resource sharing where D2D communications are allocated dedicated resources such that they can overlay cellular communications. Owing to the potential of achieving spectrum reuse, non-orthogonal resource sharing has received considerable interest; however, orthogonal sharing allows interference decoupling between D2D and cellular transmissions [140].

There has been considerable interest in TPC techniques for D2D underlying cellular networks when non-orthogonal resource sharing is used [141, 142, 143, 144]. Statistics of an SINR with simple TPC have been addressed in [141]. Radio resource management principles were designed, allowing D2Ds to flexibly select their operation bandwidth, thereby avoiding heavily interfering cellular transmissions. In [143], TPC algorithms working against co-channel cellular-D2D interference were studied.

5.2.2 Open Loop Transmission Power Control in Cellular systems

D2D communication happens within a cellular system. We concentrate on situations where uplink resources are used for D2D. In that case, one has to take into account the cellular power control principle applied by the cellular uplink users.

TPC, broadly speaking, is the intelligent selection of output power levels of transmitters with the objective of improving system capacity, coverage and QoS while reducing power consumption. To achieve these objectives, TPC mechanisms typically aim at maximizing the received power of the desired signals while limiting the interference exposed to the neighbors. In cellular and ad-hoc networks, TPC helps to ensure efficient spectral reuse and a desirable user experience by coordinating interference. On the other hand, for nodes operating on a small energy budget, energy conservation is crucial to the lifetime of the nodes and the network as a whole, and TPC minimizes the overall energy expenditure.

Usage of an orthogonal transmission scheme eliminates intra-cell interference between users in the same cell and near-far problem as of typical CDMA systems. However, since the transmission in the neighboring cell is not orthogonal, there is inter-cell interference between users in the neighboring cells that ultimately limits system performance. In order to maximize spectral efficiency, 3GPP LTE is designed for frequency reuse 1 [145] both for downlink and uplink, thus, both data and control channels are sensitive to inter-cell interference. The cell edge performance and the capacity of a cell site can be limited by the inter-cell interference. Therefore, the role of recent TPC schemes become decisive in providing the required SINR to maintain an acceptable level of communication between the base station and the user while simultaneously controlling the interference affecting neighboring cells. Therefore, 3GPP has recently proposed the use of FPC [146] to minimize the amount of harm to the neighboring cell.

This new proposal causes users with a higher path-loss to operate at a lower SINR requirement so that they will be more likely to generate less interference in neighboring cells. The recently agreed FPC scheme [146] for the Physical Uplink Shared Channel (PUSCH) is based on an Open-Loop Power Control (OLPC) algorithm, the aim of which is to compensate only for slow channel variations. In order to adapt to changes in the inter-

cell interference situation or to correct the path-loss measurements and power amplifier errors, aperiodic close-loop adjustments can also be applied. The user transmit power, expressed in dBm, is set as [146]

$$P = \min\{P_{max}, P_0 + 10\log_{10} M + \alpha PL + \Delta_{mcs} + f(\Delta_i)\} \ , \tag{5.2}$$

where P_{max} is the maximum transmit power of the user, P_0 is the target received power, M is the number of assigned Physical Resource Blocks (PRBs) of the user of interest, α is the cell-specific path-loss compensation factor, PL is the downlink path-loss measured at the user terminal based on the transmit power of the reference symbols, Δ_{mcs} is a user-specific parameter assigned by upper-layers, and Δ_i is a user-specific correction value with a relative or absolute increase depending on the function $f()$. Furthermore, the transmit power in (5.2) is simplified for a given PRB as [147]

$$P = \min\{P_{max}, P_0 + \alpha PL\} \tag{5.3}$$

by concentrating the performance of OLPC only. The performance of the fractional path loss compensation combined with OLPC is discussed in [147, 148]. FPC for interference management in OFDMA is investigated in [149, 150, 40].

5.2.3 I/Q Near-Far Effect in D2D Communication

Due to impairments in RF circuits, FDMA suffers from adjacent channel leakage and accordingly from a near-far effect. This effect is not as damaging as in a CDMA system, where the near-far-effect is seen in co-channel interference [142]. Nevertheless, LTE uplink transmission powers have to be controlled with a fair accuracy. With RF impairments, managing intra-cell orthogonality becomes an objective for TPC when using orthogonal D2D. Due to the mirror carrier interference caused by I/Q imbalance a cellular uplink transmission may create interference in the D2D reception. The severity of the performance degradation of the D2D reception can be characterized by the location of the cellular user. D2D pairs with weak SINRs scheduled on a given channel suffer more from I/Q induced cellular interference on the mirror, and an *I/Q near-far effect* can be observed.

We consider an uplink cellular infrastructure network based on OFDMA, or Single Carrier-Frequency Division Multiple Access (SC-FDMA). In addition to cellular uplink transmissions, there are D2D connections inside

a cell. For simplicity, D2D and cellular users share resources orthogonally by FDMA. D2D communication requiring orthogonal resources may be present for two reasons. Some D2D links are not able to avoid co-channel interference from cellular transmission, due to the position of the nodes, or due to the long delays in control signaling incurred by interference avoidance protocols of the kind discussed in [142]. Otherwise, the system may be designed solely for orthogonal D2D. In both cellular uplink and D2D transmissions, RF-filters are for the full system bandwidth, and a part of this bandwidth is used for transmission by an individual device. There is a cyclic prefix keeping different FDMA resources orthogonal, up to effects caused by excessive time dispersion, frequency dispersion, and RF impairments.

As in [143], all transmissions obey the same cellular power control principle, to keep the interference levels at the BS under control. Such a principle solves the two objectives of cellular power control—it keeps the inter-cell interference on a controlled level, and keep the in-cell FDMA channels approximately orthogonal at the BS receiver. Note that CSI of the link between the cellular transmitter and D2D receiver is generically not known, and does not affect the power control. In fact, to manage the dual targets of inter-cell interference control and intra-cell orthogonality at the BS, this CSI is not needed.

We focus on the cases where two transmissions occupy mirror frequency resources to highlight the effect of I/Q interference. This is a common case when there is full load in the cell so that all resources are used. The only situation where a D2D transmission would not suffer from I/Q interference of the type discussed here is when an individual D2D link occupies mirror frequency resources. In a multiuser system, inter-carrier I/Q interference results in significant interference from cellular transmission to D2D, if the D2D receiver is close to the cellular user. Due to the power control principle employed here, the impact on cellular transmission from the corresponding I/Q interference from D2D transmissions is relatively small—it is of the same size as the interference from an normal uplink transmission would be. This interference is managed by the cellular TPC method in use. Thus we focus on the cellular interference experienced by the D2D receiver.

A communication instance in the studied system is depicted in Figure. 5.3. There is one cellular user, $\mathrm{UE_c}$ and two D2D users $\mathrm{UE_{di}},\ i = 1, 2$. D2D communication happens on a mirror frequency of cellular communi-

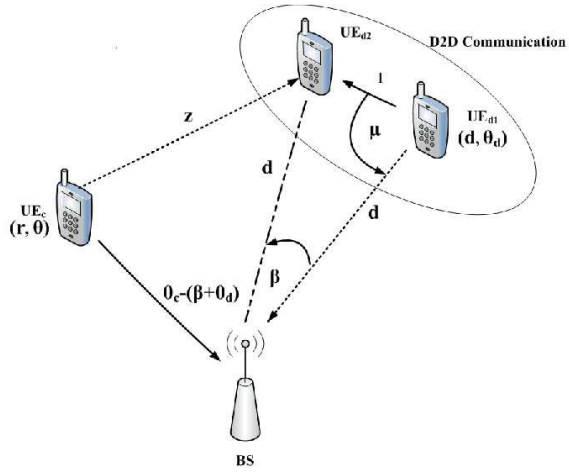

Figure 5.3. Cellular transmission with D2D communication. Desired and interference channels are shown in solid and dashed lines, respectively.

cation. This simplified scenario would be realized, for example, if orthogonal resource allocation is used in the cell, and there is an interference coupling between two resources, such as one given by I/Q imbalance.

The location of the cellular user is expressed in polar coordinates by (r, θ). The associated D2D transceiver pair is located at a fixed distance d away from the BS. The corresponding D2D receiver $\mathrm{UE_{d2}}$ is located at distance l from its transmitter, at an angle μ from the vector pointing to the base station. Note that a single cell is considered. To guarantee normal performance of the cellular system, all transmitters adjust their transmit powers according to the FPC algorithm detailed below.

Note that the I/Q interference experienced by $\mathrm{UE_{d2}}$ would be the same even if $\mathrm{UE_c}$ would be a D2D transmitter to some other D2D receiver. In that case, this second D2D transmitter might also suffer from interference from $\mathrm{UE_{d1}}$. This interference would be statistically similar to the interference experienced by $\mathrm{UE_{d2}}$ in Figure. 5.3. Thus in a situation where all FDMA resources in a cell are orthogonally distributed, it is sufficient to analyze the situation of Figure. 5.3.

Due to the geometry, the distance z that the cellular interference propagates over is variable. This distance is difficult to measure and such a measurement is not supported by current LTE specifications. Thus we will assume that information on the link between the cellular transmitter and D2D receiver is not known. This causes an IQ near far effect:

the interference at the D2D receiver varies in an uncontrolled manner according to the user scheduled on the mirror carrier. As a result, the D2D receiver may be in outage, if the cellular transmitter happens to be close to the D2D receiver. The received SINR of user $\mathrm{UE_{d1}}$ suffering from cellular interference I_c is

$$\gamma_d = \frac{\eta d^{\alpha\lambda} l^{-\lambda} |h_{d,m}|^2}{|\epsilon_R h_{c,m} + \epsilon_T^* h_{c,p}^*|^2 I_c + N_T} \quad . \tag{5.4}$$

If we apply a single-slope path loss model of the form $PL = k_0 r^\lambda$ and the FPC of (5.3), we have $\eta = p_0 k_0^{\alpha-1}$. Here, p_0 (P_0 in dB) is the FPC target of Equation (5.3) and k_0 (K_0 in dB) is the path loss at cell edge. The path loss exponent is denoted by λ. All distances r referred to in the context are normalized w.r.t the cell radius. The complex Gaussian valued channel gain of the cellular user on the the D2D receiver on the subcarrier of interest is $h_{c,p}$ and its mirror is $h_{c,m}$. Furthermore, $h_{d,m}$ is the channel gain between the D2D transceiver pair on the mirror subcarrier. The effects of I/Q imbalance on D2D receiver and the cellular transmitter are denoted by ϵ_R and ϵ_T, respectively. FPC is applied to D2D transmissions as well in effectively mitigating excessive interference from D2D to cellular users. The contribution of thermal noise at the receiver is N_T and the cellular interference is

$$I_c = \eta r^{\alpha\lambda} \left(d^2 + r^2 - 2rd\cos(\theta - \phi)\right)^{-\lambda/2} \quad , \tag{5.5}$$

where $\phi = \pi + \theta_d - 2\mu$.

Figure 5.4 illustrates the cumulative distribution of the SINR of D2D communications in the presence of transceiver I/Q imbalance compared with an ideal system without I/Q imbalance. The location of the D2D transceiver pair is fixed and 120° sector is considered. The D2D receiver is selected such that it lies on the center line of the sector. Instantaneous SINRs are simulated for two different values of $d = [0.4, 0.8]$ and $l = [0.1, 0.2]$ for $\alpha = 0.8$ and $\mathrm{IRR} = 25$dB. The distributions show the effect of fading on the wanted channel SINR in the ideal system while both the effects of the wanted channel $h_{d,m}$ and the I/Q interference variability affects the non-ideal curve. I/Q interference clearly increases the probability of low SINR, caused by I/Q near-far interference. Such interference is variable, and outside of the control of the D2D pair. Thus, it may lead to outage if the D2D transmissions schedule on mirror resources or else share the resources among both transmissions in a TDD manner. These results indicate that it is beneficial to take into account I/Q interference

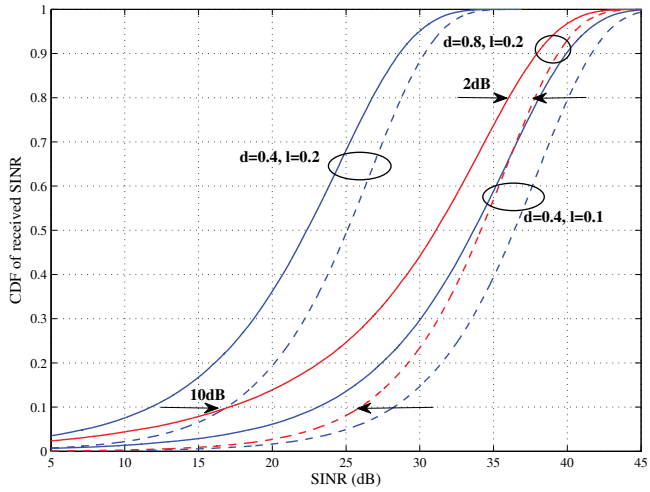

Figure 5.4. Received SINR distribution of $\mathrm{UE_{d1}}$ with (solid) and without (dashed) I/Q interference, in a 120° sector. D2D coordinates $d = [0.4,\ 0.8]$ and $l = [0.1\ 0.2]$. $\mathrm{IRR} = 25$dB is assumed for both transmitter and receiver I/Q imbalance. FPC with $\alpha = 0.8$.

when determining the resources to be used by orthogonal D2D transmissions. Further, inter-carrier I/Q interference from cellular transmission to D2D is significant, if the D2D receiver is close to the cellular user.

6. Conclusions

OFDM is the modulation technique of choice in current communications systems due to its multipath resilience and low implementation complexity. The simplest direct conversion architecture has become a widely adopted solution in designing low-cost, low-power transceiver design. However, one of the unavoidable problems associated with analog signal processing in direct conversion consists of mismatches in the gain and phases of the I and Q branches. Due to the finite tolerance of practical electronics, so-called "I/Q imbalance" introduces mirror frequency interference and degrades performance when it is not compensated. The elimination or mitigation of I/Q imbalance becomes a challenge in such communications systems while achieving performance requirements.

This thesis has considered several aspects of I/Q imbalance in systems with OFDM(A), where I/Q interference is coupling performance on mirror carrier pairs. Receiver operation, design of coding methods, and Radio Resource Management have been addressed.

CSI is crucial for data detection, channel equalization, and link adaptation. The performance of communications systems rely upon the knowledge of CSI at the receiver. The pilots and/or preambles are fundamental building blocks in practical OFDM wireless systems. The existence of such reference symbols is essential for the channel estimation and synchronization in time and frequency. I/Q imbalance directly affects the performance of estimation algorithms. Awareness of the I/Q imbalance parameter can be used to improve receiver performance. The accuracy of the I/Q imbalance parameter estimation can be significantly increased if pilot symbols are properly arranged. If a Gaussian approximation is applied to I/Q interference, good results for receiving lower-order modulation are found. For higher-order modulation, a slightly degraded performance is seen when a Gaussian approximation is used. The error floors

are slightly higher in imperfect CSI situations.

SFBC is an alternative to STBC for exploiting spatial diversity in MIMO-OFDM. In the presence of I/Q imbalance, space-frequency coding suffers from additional I/Q interference. The technique demonstrated here applies coding across mirror subcarriers based on the Alamouti scheme. It is seen that a distinguishing feature of the space-frequency coding across mirror subcarriers is that it cancels the I/Q imbalance automatically without additional signal processing, if the pilot symbols are coded also in the same manner. From the results of Paper Publication II, one learns that the lowest complexity performance for open loop diversity in channels with I/Q imbalance is provided by directly space-frequency coding across mirror subcarriers.

When CSI is available at the transmitter, linear precoding can be used to further improve system performance by tailoring the transmission to the instantaneous channel conditions while retaining the benefits of all-linear processing. Since OFDM uses multiple subcarriers, optimal precoding for MIMO-OFDM can be achieved by deriving precoders for each subcarrier independently, or for a group of adjacent subcarriers with almost identical channels. With I/Q imbalance, the signal models on mirror carrier pairs become coupled. Optimally, the precoders on a mirror carrier pair should be jointly selected. When either the subcarrier or the mirror subcarrier has a low rank transmission, the effect of precoding becomes significant. At a high SNR, where I/Q interference becomes dominant, it becomes essential to design precoders jointly.

If the transmission on the mirror subcarrier is spatially colored, the I/Q interference experienced at the subcarrier of interest becomes dependent on the link adaptation and scheduling decisions of the mirror carrier. This causes fading due to non-controlled variations in the signal quality. When the source of the interference and its statistics are known, an I/Q-aware transmitter may select an optimum transmission method to achieve performance gains. Block and ergodic fading channel models were considered. In ergodic fading, link adaptation may be performed based on statistical knowledge of the channel and the interference. The gains from I/Q awareness are limited and an I/Q-ignorant transmitter, which slightly underestimates the rate that the channel may support. In a block fading channel, link adaptation is based on the statistics of the I/Q interference, and the instantaneous fixed channel strength of the wanted transmission. The rate performance of an I/Q-aware transmission was found to outper-

form an I/Q-ignorant transmission based on an SINR-independent blind back-off. A codeword-specific SINR-dependent back-off scheme would perform almost as well as an I/Q-aware link adaptation. At high SINR and with pedestrian speeds and short delay spreads, which would be predominant in small cell networks, I/Q interference may be the dominant source of CQI errors rather than the errors induced by channel dispersion. Accordingly, I/Q aware link adaptation has significant potential in OFDMA systems.

In a hybrid network with cellular and D2D transmissions and which shared uplink mirror frequency resources, I/Q-induced interference is experienced across both transmissions. High interference peaks caused by potential cellular transmissions from the vicinity of the D2D receiver may cause outage of the D2D communications. The severity of the interference depends on the cell geometry and the location of the D2D pair in the cell. To mitigate such outages, D2D transmissions exposed to I/Q near-far effects may be allocated mirror pair resources. A simple solution to remove the I/Q-near-far effect would be to allocate cellular and D2D transmissions to different time slots. Such a solution would also automatically solve potential duplexing problems at D2D transmitters, which may need to receive control channels from the base station, while transmitting in D2D mode.

With cellular systems moving towards heterogeneity, embracing small cells and D2D, the I/Q imbalance becomes more prominent. Cheaper RF hardware may be used in small base stations, and emerging paradigms such as D2D and TDD break the strict control of uplink/downlink interference possible in cellular FDD systems. Taking I/Q interference effects into account becomes important not only when designing receiver algorithms, but also in selecting coding methods, and in radio resource management. The I/Q aware coding methods, and the I/Q flashlight and near-far effects have to be taken into account when designing future OFDM-based communication systems with hardware constraints in mind.

It is of profound importance to increase the spectral efficiency in future networks, to keep up with the increasing demand for wireless services. However, this is a challenging task and usually comes at the price of having stricter hardware and overhead requirements. As opposed to the case of ideal hardware, these practical impairments create finite ceilings on the estimation accuracy and capacity. The use of large-scale antenna arrays can bring substantial improvements in energy and/or spectral efficiency

to wireless systems due to the greatly improved spatial resolution and array gain. Despite the obvious advantages of Massive MIMO systems, one of the main drawbacks of using a great number of antennas concerns hardware imperfections in the RF links such as IQI.

Relaying-assisted transmission is considered as one of the key technologies for future wireless networks, which are capable of improving the system reliability, extending network coverage and ensuring quality of service. For such high-rate systems with low-cost relay nodes are more prone to IQI, leading to significant performance loss. Although cooperative relaying has been widely utilized in wireless communications, it simultaneously introduces a new source of security vulnerabilities to the wireless networks such as denial of service attacks. In order to minimize the potential security risks from relays, reliable relay authentication schemes become necessitated. I/Q imbalance associated with the receiving and transmission of the relaying process is considered as a unique device fingerprint for relay authentication.

References

[1] P. Rykaczewski, M. Valkama, and M. Renfors, "On the connection of I/Q imbalance and channel equalization in direct-conversion transceivers," *IEEE Trans. Vehic. Tech.*, vol. 57, no. 3, pp. 1630–1636, May 2008.

[2] S. Bassam, S. Boumaiza, and F. M. Ghannouchi, "Block-wise estimation of and compensation for I/Q imbalance in direct-conversion transmitters," *IEEE Trans. Signal Process.*, vol. 57, no. 12, pp. 4970–4973, Dec. 2009.

[3] Z. Zhu, X. Huang, and H. Leung, "Joint I/Q mismatch and distortion compensation in direct conversion transmitters," *IEEE Trans. Wireless Commun.*, vol. 12, no. 6, pp. 2841–2951, Jun. 2013.

[4] Y. Tsai, C.-P. Yen, and X. Wang, "Blind frequency-dependent I/Q imbalance compensation for direct-conversion receivers," *IEEE Trans. Wireless Commun.*, vol. 9, no. 6, pp. 1976–1986, Jun. 2010.

[5] T. C. W. Schenk, P. F. M. Smulders, and E. R. Fledderus, "Estimation and compensation of frequency selective TX/RX IQ imbalance in MIMO OFDM systems," in *Proc. IEEE International Conference on Communications (ICC)*, Jun. 2006, pp. 251–256.

[6] J. Luo, W. Keusgen, and A. Kortke, "Preamble designs for efficient joint channel and frequency-selective I/Q-imbalance compensation in MIMO OFDM systems," in *Proc. IEEE International Conference on Wireless Communications and Networking (WCNC)*, Apr. 2010, pp. 1–6.

[7] S. Traverso, M. Ariaudo, I. Fijalkow, and J.-L. Gautier, "Frequency-selective I/Q imbalance and channel estimation in OFDM receivers," in *Proc. IEEE European Conference on Wireless Technology (EuWiT)*, Oct. 2008, pp. 65–68.

[8] J. Gao, X. Zhu, H. Lin, and A. K. Nandi, "Independent component analysis based semi-blind I/Q imbalance compensation for MIMO OFDM systems," *IEEE Trans. Wireless Commun.*, vol. 9, no. 3, pp. 914–920, Mar. 2010.

[9] B. Narasimhan, S. Narayanan, N. Al-Dhahir, and H. Minn, "Digital baseband compensation of joint TX/RX frequency-dependent I/Q imbalance in mobile mimo-OFDM transceivers," in *Proc. IEEE 43rd Annual Conference on Information Sciences and Systems (CISS)*, Mar. 2009, pp. 545–550.

[10] O. Ozdemir, R. Hamila, and N. Al-Dhahir, "I/Q imbalance in multiple beamforming OFDM transceivers: SINR analysis and digital baseband

compensation," *IEEE Trans. Commun.*, vol. 61, no. 5, pp. 1914–1925, May 2013.

[11] A. Tarighat, R. Bagheri, and A. H. Sayed, "Compensation schemes and performance analysis of IQ imbalances in OFDM receivers," *IEEE Trans. Signal Process.*, vol. 53, no. 8, pp. 3257–3268, Aug. 2005.

[12] A. Schuchert, R. Hasholzner, and P. Antoine, "A novel IQ imbalance compensation scheme for the reception of OFDM signals," *IEEE Trans. Consum. Electron.*, vol. 47, no. 3, pp. 313–318, Aug. 2001.

[13] C.-P. Yen, Y. Tsai, G. Zhang, and R. Olesen, "Blind estimation and compensation of frequency-flat I/Q imbalance using cyclostationarity," in *Proc. IEEE 68th Conference on Vehicular technology (VTC)*, Sep. 2008, pp. 1–5.

[14] M. Valkama, M. Renfors, and V. Koivunen, "Blind signal estimation in conjugate signal models with application to I/Q imbalance compensation," *IEEE Signal Process. Lett.*, vol. 12, no. 11, pp. 733–736, Nov. 2005.

[15] B. S. Kirei, M. G. Neag, and M. D. Topa, "Blind frequency-selective I/Q mismatch compensation using subband processing," *IEEE Trans. Circuits Syst. II*, vol. 59, no. 5, pp. 302–306, May 2012.

[16] L. Anttila, M. Valkama, and M. Renfors, "Gradient-based blind iterative techniques for I/Q imbalance compensation in digital radio receivers," in *Proc. IEEE 8th Workshop onSignal Processing Advances in Wireless Communications (SPAWC)*, Jun. 2007, pp. 1–5.

[17] ——, "Circularity-based I/Q imbalance compensation in wideband direct-conversion receivers," *IEEE Trans. Vehic. Tech.*, vol. 57, no. 4, pp. 2009–2113, Jul. 2008.

[18] J. Tubbax, B. Come, L. V. der Perre, S. Donnay, M. Engels, H. D. Man, and M. Moonen, "Compensation of IQ imbalance and phase noise in OFDM systems," *IEEE Trans. Wireless Commun.*, vol. 4, no. 3, pp. 872–877, May 2005.

[19] Q. Zou and A. Tarighat, "Joint compensation of IQ imbalance and phase noise in OFDM wireless systems," *IEEE Trans. Commun.*, vol. 57, no. 2, pp. 404–414, Feb. 2009.

[20] N. Y. Ermolova and O. Tirkkonen, "Analysis of joint effect of nonlinear amplification and I/Q imbalance in OFDM transmission," in *Proc. IEEE 21st International Symposium on Personal Indoor and Mobile Radio Communications (PIMRC)*, Sep. 2010, pp. 656–661.

[21] M. Asim, D. McLernon, and M. Ghogho, "Receiver design for OFDM in the presence of I/Q imbalance and amplifier nonlinearity," in *Proc. IEEE Sensor Signal Processing for Defence (SSPD)*, Sep. 2012, pp. 1–5.

[22] M. Cao and H. Ge, "I/Q imbalance mitigation for STBC MIMO-OFDM communication systems," in *Proc. IEEE International Conference on Acoustics, Speech and Signal Processing (ICASSP)*, Apr. 2008, pp. 3093–3096.

[23] Y. Zou, M. Valkama, and M. Renfors, "Digital compensation of I/Q imbalance effects in space-time coded transmit diversity systems," *IEEE Trans. Signal Process.*, vol. 56, no. 6, pp. 2496–2508, Jun. 2008.

[24] M. Cao and H. Ge, "GLCP OFDM systems with I/Q imbalance," *IEEE Commun. Lett.*, vol. 13, no. 4, pp. 230–232, Apr. 2009.

[25] A. J. Grant, "Performance analysis of transmit beamforming," *IEEE Trans. Commun.*, vol. 53, no. 4, pp. 738–744, Apr. 2005.

[26] D. J. Love and R. W. Heath, "Necessary and sufficient conditions for full diversity order in correlated rayleigh fading beamforming and combining systems," *IEEE Trans. Wireless Commun.*, vol. 4, no. 1, pp. 20–23, Jan. 2005.

[27] B. Maham and O. Tirkkonen, "Impact of transceiver I/Q imbalance on transmit diversity of beamforming OFDM systems," *IEEE Trans. Commun.*, vol. 60, no. 3, pp. 643–648, Mar. 2012.

[28] M. Windisch and G. Fettweis, "On the impact of I/Q imbalance in multi-carrier systems for different channel scenarios," in *Proc. IEEE International Symposium on Circuits and Systems (ISCAS)*, May 2007, pp. 33–36.

[29] Y. Zou, M. Valkama, N. Y. Ermolova, and O. Tirkkonen, "Analytical performance of OFDM radio link under RX I/Q imbalance and frequency-selective Rayleigh fading channel," in *Proc. IEEE 12th International Workshop on Signal Processing Advances in Wireless Communications (SPAWC)*, Jun. 2011, pp. 251–255.

[30] S. Krone and G. Fettweis, "Capacity analysis for OFDM systems with transceiver I/Q imbalance," in *Proc. IEEE Global Telecommunications Conference (GLOBECOM)*, Nov. 2008, pp. 1–6.

[31] M. Windisch and G. Fettweis, "Performance degradation due to I/Q imbalance in multi-carrier direct conversion receivers: A theoretical analysis," in *Proc. IEEE International Conference on Communications (ICC)*, Jun. 2006, pp. 257–262.

[32] O. Ozdemir, R. Hamila, and N. Al-Dhahir, "SINR analysis for beamforming OFDM systems under joint transmit-receive I/Q imbalance," in *Proc. IEEE 23rd International Symposium on Personal Indoor and Mobile Radio Communications (PIMRC)*, Sep. 2012, pp. 1891–1901.

[33] J. Qi and S. Aissa, "Analysis and compensation of I/Q imbalance in MIMO transmit-receive diversity systems," *IEEE Trans. Commun.*, vol. 58, no. 5, pp. 1546–1556, May 2010.

[34] M. V. Y. Zou and M. Renfors, "Performance analysis of space-time coded MIMO-OFDM systems under I/Q imbalance," in *Proc. IEEE International Conference on Acoustics, Speech and Signal Processing (ICASSP)*, Apr. 2007, pp. 341–344.

[35] M. Krondorf and G. Fettweis, "Numerical performance evaluation for Alamouti space time coded OFDM under receiver impairments," *IEEE Trans. Wireless Commun.*, vol. 8, no. 3, pp. 1446–1455, Mar. 2009.

[36] A. Gomaa, M. Mokhtar, and N. Al-Dhahir, "Amplify-and-forward relaying under I/Q imbalance," in *Proc. IEEE Global Communications Conference (GLOBECOM)*, Dec. 2012, pp. 4761–4676.

[37] O. Semiari, B. Maham, and C. Yuen, "On the effect of I/Q imbalance on energy detection and a novel four-level hypothesis spectrum sensing," *IEEE Trans. Vehic. Tech.*, vol. 63, no. 8, pp. 4136–4141, Oct. 2014.

[38] M. Krondorf and G. Fettweis, "OFDM link performance analysis under various receiver impairments 2008:145279," *EURASIP Journal on Wireless Communication and networking.*, 2008.

[39] B. Razavi, "Design considerations for direct-conversion receivers," *IEEE Trans. Circuits Syst. II*, vol. 44, no. 6, pp. 428–435, Jun. 1997.

[40] U. Oruthota, P. Dharmawansa, and O. Tirkkonen, "Analysis of uplink power control in cellular mobile systems," in *Proc. IEEE 77th Vehicular Technology Conference (VTC)*, Jun. 2013, pp. 1–5.

[41] A. Baier, "Quadrature mixer imbalances in digital TDMA mobile radio receivers," in *Proc. Int. Zurich Seminar Digital Commun., Electronic Circuits Syst. Commun.*, May 1990, pp. 147–162.

[42] C. L. Liu, "Impacts of I/Q imbalance on QPSK-OFDM-QAM detection," *IEEE Trans. Consum. Electron.*, vol. 44, no. 3, pp. 984–989, Aug. 1998.

[43] L. Yang and K. P. J. Armstrong, "Impact of timing jitter and I/Q imbalance in OFDM systems," *IEEE Commun. Lett.*, vol. 17, no. 2, pp. 253–256, Feb. 2013.

[44] B. Narasimhan, S. Narayanan, and H. Minn, "Reduced-complexity baseband compensation of joint Tx/Rx I/Q imbalance in mobile MIMO-OFDM," *IEEE Trans. Wireless Commun.*, vol. 9, no. 5, pp. 1720–1728, May 2010.

[45] C. E. Shannon, "Communication in the presence of noise," *Proc. IEEE*, vol. 86, no. 2, pp. 447–457, Feb. 1949.

[46] A. Goldsmith, *Wireless Communications*. Cambridge University Press, 2005.

[47] S. Krone and G. Fettweis, "On the capacity of OFDM systems with receiver I/Q imbalance," in *Proc. IEEE International Conference on Communications (ICC)*, May 2008, pp. 1317–1321.

[48] B. Maham and O. Tirkkonen, "Transmit antenna selection OFDM systems with transceiver I/Q imbalance," *IEEE Trans. Vehic. Tech.*, vol. 61, no. 2, pp. 856–871, Feb. 2012.

[49] S. Fouladifard and H. Shafiee, "A new technique for estimation and compensation of IQ imbalance in OFDM receivers," in *Proc. International Conference on Communication Systems*, Nov. 2002, pp. 224–228.

[50] J. Tubbax, B. Come, L. van der Perre, L. Deneire, S. Donnay, and M. Engels, "Compensation of IQ imbalance in OFDM systems," in *Proc. IEEE International Conference on Communications (ICC)*, May 2003, pp. 3403–3407.

[51] M. Valkama, M. Renfors, and V. Koivunen, "On the performance of interference canceller based I/Q imbalance compensation," in *Proc. IEEE International Conference on Acoustics, Speech, and Signal Processing (ICASSP)*, Jun. 2000, pp. 2885–2888.

[52] K. Sung and C. Chao, "Estimation and compensation of I/Q imbalance in OFDM direct-conversion receivers," *IEEE Trans. Signal Process.*, vol. 3, no. 3, pp. 438–453, Jun. 2009.

[53] G. T. Gil, I. H. Sohn, J. K. Park, and Y. H. Lee, "Joint ML estimation of carrier frequency, channel, I/Q mismatch, and DC offset in communication receivers," *IEEE Trans. Vehic. Tech.*, vol. 54, no. 1, pp. 338–349, Jan. 2005.

[54] J. Gao, X. Zhu, H. Lin, and A. K. Nandi, "Linear least squares CFO estimation and kalman filtering based I/Q imbalance compensation in MIMO SC-FDE systems," in *Proc. IEEE International Conference on Communications (ICC)*, May 2010, pp. 1–5.

[55] S. Fouladifard and H. Shafiee, "On adaptive cancellation of IQ mismatch in OFDM receivers," in *Proc. IEEE International Conference on Acoustics, Speech and Signal Processing*, Apr. 2003, pp. 564–567.

[56] B. S. Kirei, M. Neag, and M.D.Topa, "Symmetric adaptive decorrelation for I/Q imbalance compensation in narrowband receivers," in *Proc. IEEE 9th International Symposium on Electronics and Telecommunications (ISETC)*, Nov. 2010, pp. 353–356.

[57] G. Xing, M. Shen, and H. Liu, "Frequency offset and I/Q imbalance compensation for direct-conversion receivers," *IEEE Trans. Wireless Commun.*, vol. 4, no. 2, pp. 673–680, Mar. 2005.

[58] E. Lopez-Estraviz, S. D. Rore, F. Horlin, and A. Bourdoux, "Pilot design for joint channel and frequency-dependent transmit/receive IQ imbalance estimation and compensation in OFDM-based transceivers," in *Proc. IEEE Eleventh International Conference on Communications (ICC)*, Jun. 2007, pp. 4861–4866.

[59] H. Minn and D. Munoz, "Effect of I/Q imbalance on pilot design for MIMO OFDM channel estimation," in *Proc. IEEE Global Telecommunications Conference (GLOBECOM)*, Nov. 2010, pp. 1–5.

[60] Y. Egashira, Y. Tanabe, and K. Sato, "A novel IQ imbalance compensation method with pilot-signals for OFDM system," in *Proc. IEEE 64th Vehicular Technology Conference (VTC)*, Sep. 2006, pp. 1–5.

[61] P. Michael, H. Werner, and S. Andreas, "Blind compensation of I/Q filter imbalance in the LTE downlink," in *Proc. IEEE 11th Europian Conference on Sustainable Wireless Technologies*, Apr. 2011, pp. 1–7.

[62] H. Lin and K.Yamashita, "Blind frequency-dependent I/Q imbalance compensation using system identification," in *Proc. IEEE Conference on Global Telecommunications (GLOBECOM)*, Dec. 2011, pp. 1–5.

[63] L. Anttila, M. Valkama, and M. Renfors, "Blind compensation of frequency-selective I/Q imbalances in quadrature radio receivers: Circularity -based approach," in *Proc. IEEE International Conference on Acoustics, Speech and Signal Processing (ICASSP)*, Apr. 2007, pp. 245–248.

[64] ——, "Frequency-selective I/Q mismatch calibration of wideband direct-conversion transmitters," *IEEE Trans. Circuits Syst. II*, vol. 55, no. 4, pp. 359–363, Apr. 2008.

[65] R. K. McPherson, "Frequency-selective I/Q imbalance compensation for OFDM transmitters using online frequency-domain adaptive predistortion," in *Proc. IEEE Military Communications Conference (MILCOM)*, Nov. 2011, pp. 532–537.

[66] Y. Zou, M. Valkama, and M. Renfors, "Pilot-based compensation of frequency-selective I/Q imbalances in direct-conversion OFDM transmitters," in *Proc. IEEE Vehicular Technology Conference (VTC)*, Sep. 2008, pp. 1–5.

[67] M. Valkama, M. Renfors, and V. Koivunen, "Advanced methods for I/Q imbalance compensation in communication receivers," *IEEE Trans. Signal Process.*, vol. 49, no. 10, pp. 2335–2344, Oct. 2001.

[68] T. L. Marzetta and B. M. Hochwald, "Capacity of a mobile multiple-antenna communication link in Rayleigh flat fading," *IEEE Trans. Inf. Theory*, vol. 45, no. 1, pp. 139–157, Jan. 1999.

[69] A. Goldsmith, S. A. Jafar, N. Jindal, and S. Vishwanath, "Capacity limits of MIMO channels," *IEEE J. Sel. Areas Commun.*, vol. 21, no. 5, pp. 684–702, Jun. 2003.

[70] S. Zhou and G. B. Giannakis, "Finite-alphabet based channel estimation for OFDM and related multicarrier systems," *IEEE Trans. Commun.*, vol. 49, no. 8, pp. 1402–1414, Aug. 2001.

[71] H. Bolcskei, J. R.W. Heath, and A. J. Paulraj, "Blind channel identification and equalization in OFDM-based multi-antenna systems," *IEEE Trans. Signal Process.*, vol. 50, no. 1, pp. 96–109, Jan. 2002.

[72] R. Negi and J. Cioffi, "Pilot tone selection for channel estimation in a mobile OFDM system," *IEEE Trans. Consum. Electron.*, vol. 44, no. 3, pp. 1112–1128, Aug. 1998.

[73] I. Barhumi, G. Leus, and M. Moonen, "Optimal training design for MIMO OFDM systems in mobile wireless channels," *IEEE Trans. Signal Process.*, vol. 51, no. 6, pp. 1615–1642, Jun. 2003.

[74] S. Ohno and G. B. Giannakis, "Optimal training and redundant precoding for block transmissions with applications to wireless OFDM," in *Proc. IEEE International Conference on Acoustics, Speech, and Signal Processing (ICASSP)*, May 2001, pp. 2389–2392.

[75] O. Edfors, M. Sandell, J. J. V. de Beek, S. K. Wilson, and P. O. Borjesson, "OFDM channel estimation by singular value decomposition," *IEEE Trans. Commun.*, vol. 46, no. 7, pp. 931–939, Jul. 1998.

[76] L. Deneire, P. Vandenameele, L. V. der Perre, B. Gyselinckx, and M. Engels, "A low complexity ML channel estimator for OFDM," in *Proc. IEEE International Conference in Communications*, Jun. 2001, pp. 11–14.

[77] P. Rabiei, W. Namgoong, and N. Al-Dhahir, "Reduced-complexity joint baseband compensation of phase noise and I/Q imbalance for MIMO-OFDM systems," *IEEE Trans. Wireless Commun.*, vol. 9, no. 11, pp. 3450–3460, Nov. 2010.

[78] H. Minn and N. Al-Dhahir, "Optimal training signals for MIMO OFDM channel estimation," *IEEE Trans. Wireless Commun.*, vol. 5, no. 5, pp. 1158–1168, May 2006.

[79] L. Brotje, S. Vogeler, and K. D. Kammeyer, "Estimation and correction of transmitter-caused I/Q imbalance in ofdm systems," in *Proc. 7th International OFDM-Workshop (InOWo)*, Sep. 2002, pp. 1–5.

[80] T. M. Ylämurto, "Frequency domain IQ imbalance correction scheme for orthogonal frequency division multiplexing (OFDM) systems," in *Proc. IEEE International Conference on Wireless Communications and Networking (WCNC)*, Mar. 2003, pp. 20–25.

[81] M. Windisch and G. Fettweis, "Preamble design for an efficient I/Q imbalance compensation in OFDM direct-conversion receivers," in *Proc. IEEE 10th International OFDM Workshop*, Sep. 2005, pp. 1–5.

[82] J. Y. Yu, M. F. Sun, T. Y. Hsu, and C. Y. Lee, "A novel technique for I/Q imbalance and CFO compensation in OFDM systems," in *Proc. IEEE International Symposium on Circuits and Systems (ISCS)*, May 2005, pp. 6030–6033.

[83] IEEE 802.11g, "Supplement to standard for LAN/MAN part 11: Wireless mac and phy specifications: Further higher data rate extension in the 2.4GHz band," 2003.

[84] H. Minn and D. Munoz, "Pilot designs for channel estimation of OFDM systems with frequency-dependent I/Q imbalances," in *Proc. IEEE Wireless Communications and Networking Conference (WCNC)*, Apr. 2009, pp. 1–6.

[85] S. Narayanan, B. Narasimhan, and N. Al-Dhahir, "Training sequence design for joint channel and I/Q imbalance parameter estimation in mobile SC-FDE transceivers," in *Proc. IEEE International Conference on Acoustics Speech and Signal Processing (ICASSP)*, Mar. 2010, pp. 3186–3189.

[86] E. Manasseh, S. Ohno, and M. Nakamoto, "Training symbol design for channel estimation and IQ imbalance compensation in OFDM systems," in *Proc. IEEE 75th Vehicular Technology Conference (VTC)*, May 2012, pp. 1–5.

[87] M. Windisch and G. Fettweis, "Standard-independent I/Q imbalance compensation in OFDM direct-conversion receivers," in *Proc. IEEE International OFDM Workshop*, vol. 53, no. 9, Sep. 2004, pp. 57–61.

[88] ——, "Blind estimation and compensation of I/Q imbalance in OFDM receivers with enhancements through Kalman filtering," in *Proc IEEE 14th Workshop on Statistical Signal Processing (SSP)*, Aug. 2007, pp. 754–758.

[89] M. K. Simon and M.-S. Alouini, *Digital Communications Over Fading Channels: A Unified Approach to Performance Analysis*. Hoboken, NJ: Wiley, 2000.

[90] G. Stuber, *Principles of Mobile Communications 2nd ed.* Norwell, MA: Kluwer, 2003.

[91] A. Goldsmith and S. G. Chua, "Variable-rate variable-power M-QAM for fading channels," *IEEE Trans. Commun.*, vol. 45, no. 10, pp. 1218–1230, Oct. 1997.

[92] Y. Ma, R. Schober, and S. Pasupathy, "Performance of M-PSK with GSC and EGC with Gaussian weighting errors," *IEEE Trans. Vehic. Tech.*, vol. 54, no. 1, pp. 149–162, Jan. 2005.

[93] X. Cai and G. B. Giannakis, "Adaptive PSAM accounting for channel estimation and prediction errors," *IEEE Trans. Wireless Commun.*, vol. 4, no. 1, pp. 246–256, Jan. 2005.

[94] Y. Ma and J. Jin, "Effect of channel estimation errors on M-QAM with MRC and EGC in Nakagami fading channels," *IEEE Trans. Vehic. Tech.*, vol. 56, no. 3, pp. 1239–1250, May 2007.

[95] H. Jafarkhani, *Space-Time Coding, 1st ed.* Cambridge University Press, 2005.

[96] E. Telatar, "Capacity of multi-antenna Gaussian channels," *AT&T-Bell Laboratories Internal Tech. Memo*, Jun. 1995.

[97] A. Scaglione, P. Stoica, S. Barbarossa, G. B. Giannakis, and H. Sampath, "Optimal designs for space-time linear precoders and decoders," *IEEE Trans. Signal Process.*, vol. 50, no. 5, pp. 1051–1064, May 2002.

[98] A. M. Khachan, A. J. Tenenbaum, and R. S. Adve, "Linear processing for the downlink in multiuser MIMO systems with mutiple data streams," in *Proc. IEEE International Conference on Communications (ICC)*, Jun. 2006, pp. 4113–4118.

[99] A. Narula, M. D. Trott, and G. W. Wornell, "Performance limits of coded diversity methods for transmitter antenna arrays," *IEEE Trans. Inf. Theory*, vol. 45, no. 7, pp. 2418–2433, Nov. 1999.

[100] T. Pande, D. J. Love, and J. V. Krogmeier, "Reduced feedback MIMO-OFDM precoding and antenna selection signal processing," *IEEE Trans. Signal Process.*, vol. 55, no. 5, pp. 2284–2293, May 2007.

[101] H. Sampath and A. J. Paulraj, "Joint transmit and receive optimization for high data-rate wireless communication using multiple antennas," in *Proc. IEEE Asilomar Conference on Signals, Systems and Computers*, Oct. 1999, pp. 215–219.

[102] V. Tarokh, N. Seshadri, and A. Calderbank, "Space-time codes for high data rate wireless communication: performance criterion and code construction," *IEEE Trans. Inf. Theory*, vol. 44, no. 2, pp. 744–765, Jul. 1998.

[103] S. Alamouti, "A simple transmit diversity technique for wireless communications," *IEEE J. Sel. Areas Commun.*, vol. 16, no. 8, pp. 1451–1548, Oct. 1998.

[104] M. Valkama, Y. Zou, and M. Renfors, "On I/Q imbalance effects in MIMO space-time coded transmission systems," in *Proc. IEEE Radio and Wireless Symposium*, Jan. 2006, pp. 223–226.

[105] Y. Zou, M. Valkama, and M. Renfors, "Compensation of frequency-selective I/Q imbalances in space-time coded multi-antenna OFDM systems," in *Proc. IEEE 3rd International Symposium on Communications, Control and Signal Processing (ISCCSP)*, Mar. 2008, pp. 123–128.

[106] D. Agrawal, V. Tarokh, A. Naguib, and N. Seshadri, "Space-time coded OFDM for high data-rate wireless communication over wideband channels," in *Proc. IEEE 48th Vehicular Technology Conference (VTC)*, May 1998, pp. 2232–2236.

[107] K. F. Lee and D. B. Williams, "A space-frequency transmitter diversity technique for OFDM systems," in *Proc. IEEE Global Telecommunications Conference (GLOBECOM)*, Nov. 2000, pp. 1473–1477.

[108] J. Lee, J. Han, and J. Zhang, "MIMO technologies in 3GPP LTE and LTE-Advanced 2009:302092," *EURASIP Journal on Wireless Communication and networking.*, 2009.

[109] H. Bolcskei and A. J. Paulraj, "Space-frequency coded broadband OFDM systems," in *Proc. IEEE Wireless Communications and Networking Conference (WCNC)*, Sep. 2000, pp. 1–6.

[110] ——, "Space-frequency codes for broadband fading channels," in *Proc. IEEE International Symposium on Information Theory (ISIT)*, Jun. 2001, pp. 1–5.

[111] B. Lu and X. Wang, "Space-time code design in OFDM systems," in *Proc. IEEE Global Telecommunication Conference (GLOBECOM)*, Nov. 2000, pp. 1000–1004.

[112] Y. Tanabe, Y. Egashira, T. Aoki, and K. Sato, "Suitable MIMO-OFDM decoders to compensate IQ imbalance," in *Proc. IEEE Wireless Communications and Networking Conference (WCNC)*, Mar. 2007, pp. 863–868.

[113] Z. Shen, J. Andrews, and B. Evans, "Adaptive resource allocation in multiuser OFDM systems with proportional rate constraints," *IEEE Trans. Wireless Commun.*, vol. 4, no. 6, pp. 2726–2737, Nov. 2005.

[114] M. Moretti and A. Perez-Neira, "Efficient margin adaptive acheduling for MIMO-OFDMA systems," *IEEE Trans. Wireless Commun.*, vol. 12, no. 1, pp. 278–287, Dec. 2012.

[115] H. Dahrouj, E. S. R. Sr., and W. Yu, "Coordinated beamforming for the multi-cell multi-antenna wireless wystem," *IEEE Trans. Wireless Commun.*, vol. 9, no. 5, pp. 1748–1759, May 2010.

[116] C.-B. Chae, I. Hwang, R. Heath, and V. Tarokh, "Interference aware-coordinated beamform system in a two-cell environment," *IEEE Trans. Wireless Commun.*, vol. 11, pp. 3692–3703, Oct. 2012.

[117] E. A. Jorswieck, E. G. Larsson, and D. Danev, "Complete characterization of the pareto boundary for the MISO interference channel," *IEEE Trans. Signal Process.*, vol. 56, no. 10, pp. 5292–5296, Oct. 2008.

[118] A. Hjorungnes, *Complex-Valued Matrix Derivatives with Applications in Signal Processing and Communications*. Cambridge University Press, 2011.

[119] A. Maharshi, L. Tong, and A. Swami, "Cross-layer designs of multichannel reservation MAC under Rayleigh fading," *IEEE Trans. Signal Process.*, vol. 51, no. 8, pp. 2054–2067, Aug. 2003.

[120] X. Wang and J. K. Tugnait, "A bit-map-assisted dynamic queue protocol for multi-access wireless networks with multiple packet reception," *IEEE Trans. Signal Process.*, vol. 51, no. 8, pp. 2068–2081, Aug. 2003.

[121] G. Song and L. Ye, "Utility-based resource allocation and scheduling in OFDM-based wireless broadband networks," *IEEE Commun. Lett.*, vol. 43, no. 12, pp. 127–134, Dec. 2005.

[122] B. Vucetic, "An adaptive coding scheme for time-varying channels," *IEEE Trans. Commun.*, vol. 39, no. 5, pp. 653–663, May 1991.

[123] A. Goldsmith and S. G. Chua, "Variable-rate variable-power MQAM for fading channels," *IEEE Trans. Commun.*, vol. 45, no. 10, pp. 1218–1230, Oct. 1997.

[124] S. Alamouti and S. Kallel, "Adaptive trellis-coded multiple-phase-shift keying for Rayleigh fading channels," *IEEE Trans. Commun.*, vol. 42, no. 6, pp. 2305–2314, Jun. 1994.

[125] T. L. Jensen, S. Kant, J. Wehinger, and B. H. Fleury, "Fast link adaptation for MIMO OFDM," *IEEE Trans. Vehic. Tech.*, vol. 59, no. 8, pp. 3766–3778, Oct. 2010.

[126] M. Miyashita, M. Mikami, and H. Yoshino, "An MMI based adaptive modulation and coding for cooperative MIMO-OFDM in frequency selective channels," in *Proc. IEEE International Symposium on Antennas and Propagation (ISAP)*, Oct. 2012, pp. 738–741.

[127] S. B. Wicker, *Error Control Systems for Digital communication and Storage*. NJ: Prentice-Hall, 1995.

[128] M. Munster, T. Keller, and L. Hanzo, "Co-channel interference suppression assisted adaptive OFDM in interference limited environments," in *Proc. IEEE 49th Conference on Vehicular technology (VTC)*, Sep. 1999, pp. 284–288.

[129] L. Toni, A. Conti, M. Chiani, and O. Andrisano, "Adaptive modulation systems subject to interference," in *6th Karlsruhe Workshop on Software Radios, Universitaet Karlsruhe (TH)*, 2010, pp. 1–6.

[130] M. Taki and F. Lahouti, "Discrete rate interfering cognitive link adaptation design with primary link spectral efficiency provisioning," *IEEE Trans. Wireless Commun.*, vol. 10, no. 9, pp. 2929–2939, Sep. 2011.

[131] L. Musavian, S. Aissa, and S. Lambotharan, "Adaptive modulation in spectrum-sharing channels under delay quality-of-service constraints," *IEEE Trans. Vehic. Tech.*, vol. 60, no. 3, pp. 901–911, Mar. 2011.

[132] J. Kurjenniemi, T. Nihtilä, E. Virtej, and T. Ristaniemi, "On the effect of reduced interference predictability to the HSDPA network performance with closed loop transmit diversity," in *Proc. Internat. Symp. on Wireless Personal Multimedia Commun. (WPMC)*, Sep. 2006, pp. 864–868.

[133] C.-H. Yu, A. Hellsten, and O. Tirkkonen, "Rate adaptation of AMC/HARQ systems with CQI errors," in *Proc. IEEE 71st Vehicular Technology Conference (VTC)*, May 2010, pp. 1–5.

[134] S. Falahati, A. Svensson, M. Sternad, and T. Ekman, "Adaptive modulation systems for predicted wireless channels," *IEEE Trans. Commun.*, vol. 52, no. 2, pp. 307–316, Mar. 2004.

[135] D. L. Goeckel, "Adaptive coding for time-varying channels using outdated fading estimates," *IEEE Trans. Commun.*, vol. 47, no. 6, pp. 844–855, Jun. 1999.

[136] S. H. Park, J. W. Kim, and C. G. Kang, "Design of adaptive modulation and coding scheme for truncated HARQ," in *Proc. IEEE 2nd International Symposium on Wireless Pervasive Computing (ISWPC)*, Feb. 2007, pp. 151–155.

[137] T. Peng, Q. Lu, H. Wang, S. Xu, and W. Wang, "Interference avoidance mechanisms in the hybrid cellular and device-to-device systems," in *Proc. IEEE 20th International Symposium on Personal, Indoor and Mobile Radio Communications (PIMRC)*, Sep. 2009, pp. 617–621.

[138] C.-H. Yu, O. Tirkkonen, K. Doppler, and C. Ribeiro, "Power optimization of device-to-device communication underlaying cellular communication," in *Proc. IEEE International Conference on Communications (ICC)*, Jun. 2009, pp. 1–5.

[139] P. Janis, V. Koivunen, C. Ribeiro, K. Doppler, and K. Hugl, "Interference-avoiding MIMO schemes for device-to-device radio underlaying cellular networks," in *Proc. IEEE 20th International Symposium on Personal, Indoor and Mobile Radio Communications (PIMRC)*, Sep. 2009, pp. 2385–2389.

[140] K. Doppler, C.-H. Yu, C. Ribeiro, and P. Janis, "Mode selection for device-to-device communication underlaying an LTE-Advanced network," in *Proc. IEEE Wireless Communications and Networking Conference (WCNC)*, Apr. 2010, pp. 1–6.

[141] C.-H. Yu, O. Tirkkonen, K. Doppler, and C. Ribeiro, "On the performance of device-to-device underlay communication with simple power control," in *Proc. IEEE 69th Vehicular Technology Conference (VTC)*, Apr. 2009, pp. 1–5.

[142] S. Xu, H. Wang, T. Chen, Q. Huang, and T. Peng, "Effective interference cancellation scheme for device-to-device communication underlaying cellular networks," in *Proc. IEEE 72nd Vehicular Technology Conference (VTC)*, Sep. 2010, pp. 1–5.

[143] H. Xing and S. Hakola, "The investigation of power control schemes for a device-to-device communication integrated into OFDMA cellular system," in *Proc. IEEE 21st International Symposium on Personal Indoor and Mobile Radio Communications (PIMRC)*, Sep. 2010, pp. 1775–1780.

[144] X. Xiao, X. Tao, and J. Lu, "A QoS-aware power optimization scheme in OFDMA systems with integrated device-to-device (D2D) communications," in *Proc. IEEE 52th Vehicular Technology Conference (VTC)*, Sep. 2011, pp. 1–5.

[145] 3GPP; TSG RAN, "E-UTRA physical layer procedures," TS 36.213 V8.8.0, 2009.

[146] ——, "Way forward on power control of PUSCH," R1-073224, Jun. 2007.

[147] C. U. Castellanos, D. Villa, C. Rosa, K. I. Pedersen, F. Calabrese, P.-H. Michaelsen, and J. Michel, "Performance of uplink fractional power control in UTRAN LTE," in *Proc. IEEE 67th Vehicular Technology Conference (VTC)*, May 2008, pp. 2517–2521.

[148] A. Simonsson and A. Furuskar, "Uplink power control in LTE - overview and performance, subtitle: Principles and benefits of utilizing rather than compensating for SINR variations," in *Proc. IEEE 68th Vehicular Technology Conference (VTC)*, Sep. 2008, pp. 1–5.

[149] A. M. Rao, "Reverse link power control for managing inter-cell interference in orthogonal multiple access systems," in *Proc. IEEE 65th Vehicular Technology Conference (VTC)*, Sep. 2007, pp. 1837–1841.

[150] M. Coupechoux and J. M. Kelif, "How to set the fractional power control compensation factor in LTE?" in *Proc. IEEE 34th Sarnoff Symposium*, May 2011, pp. 1–5.

Aalto-DD 219/2015

ISBN 978-952-60-6595-3 (printed)
ISBN 978-952-60-6596-0 (pdf)
ISSN-L 1799-4934
ISSN 1799-4934 (printed)
ISSN 1799-4942 (pdf)

Aalto University
School of Electrical Engineering
Department of Communications and Networking
www.aalto.fi

BUSINESS + ECONOMY

ART + DESIGN + ARCHITECTURE

SCIENCE + TECHNOLOGY

CROSSOVER

DOCTORAL DISSERTATIONS